

**PHOTOPHYSICOCHEMICAL
PROPERTIES OF ALUMINIUM
PHTHALOCYANINE -PLATINUM
CONJUGATES.**

A thesis submitted in fulfilment of the requirements for the degree of

MASTER OF SCIENCE

Of

RHODES UNIVERSITY

By

NDUDUZO NKANYISO MALINGA

FEBRUARY 2013

DEDICATION

TO

My Parents:

Sibusiso and Gabsile Malinga

For the love, support and encouragement.

My Siblings

Khethiwe, Thabsile and Ndumiso,

ACKNOWLEDGEMENTS

“For you have formed my inward parts: you have covered me in my mother’s womb.” Psalm 139: 13

To Him who raised Jesus from the dead, to Jesus the Word of God creator of all things visible and invisible, to Holy Spirit the mighty Force of God. I give my thanks to the Holy Trinity, God almighty for source life, inspiration and for the divine protection.

My deepest gratitude goes to my supervisor Prof Tebello Nyokong. Thank you taking me into your research group and for the opportunities given to me. Thanks for the opportunity to go do some of my research in the Organic Intermediates and Dyes Institute, Moscow. I give my thanks to Drs’ Nina Kuznetsova and Olga Dolotova my host supervisors. I give my gratitude to Dr Edith Antunes for all the support, guidance and motivation throughout the two years. And to my brothers and sisters of S22, thanks for getting through the craziest two years of my life.

Thanks to the Department of Science and Technology (DST) and National Research Foundation (NRF) South Africa through DST/NRF South African Research Chairs Initiative for Professor of Medicinal Chemistry and Nanotechnology and Rhodes University for the financial support.

ABSTRACT

The combination of chemotherapy and photodynamic therapy was investigated by synthesis and characterization of octacarboxy phthalocyanine covalent conjugates with platinum complexes. This work presents the synthesis, characterization and photophysical properties of aluminium (diaquaplatinum) octacarboxyphthalocyanine and aluminium (diammine) octacarboxyphthalocyanine. The conjugates were prepared by conjugating aluminium octacarboxy phthalocyanine with potassium tetrachloro platinate to yield aluminium tetrakis and tris (diaquaplatinum) octacarboxy phthalocyanine. The aluminium octacarboxy phthalocyanine was also conjugated with cis-diamminedichloroplatinum to yield aluminium bis and tris (diaquaplatinum) octacarboxy phthalocyanine. From the characterization of the conjugates it was discovered that the aluminium (diaquaplatinum) octacarboxy phthalocyanine had formed platinum nanoparticles with the Pc acting as a capping agent. The triplet lifetimes decreased with the increasing number of platinum complexes conjugated to the Pc. The heavy atom effect improved the overall photophysical properties.

TABLE OF CONTENTS

Title page	i
Dedication	ii
Acknowledgements	iii
Table of contents	v
List of Abbreviations	viii
List of Symbols	ix
List of Schemes	xi
List of Figures	xii
List of Tables	xvi
1. Introduction	1
1.1 Some methods used in cancer therapy	2
1.1.1 Mechanism of photodynamic therapy	3
1.1.2 Chemotherapy based on platinum drugs	7
1.2 Chemistry of phthalocyanines	9
1.2.1 History and structure of phthalocyanines	9
1.2.2 Phthalocyanine synthesis	11
1.2.2.1 Symmetrical phthalocyanines	11
1.2.2.2 Synthesis of symmetrically octasubstituted phthalocyanines	13

1.2.2.3	Synthesis of octacarboxyphthalocyanines	14
1.2.2.4	Phthalocyanine used in this work	15
1.2.3	Absorption spectra of phthalocyanine	16
1.2.4	Photophysical and photochemical parameters	19
1.2.4.1	Photophysical parameters	19
1.2.4.2	Fluorescence quantum yields and lifetimes	21
1.2.4.3	Triplet quantum yields and lifetimes	23
1.2.4.4	Singlet oxygen quantum yield	26
1.2.4.5	Photodegradation/Photobleaching	28
1.3	Covalent phthalocyanine conjugates	31
1.4	Summary of aims	33
2.	Experimental	34
2.1	Materials	35
2.2	Equipment and instrumental	36
2.3	Methods	40
2.3.1	Fluorescence and triplet quantum yields and lifetimes	40
2.3.2	Singlet oxygen	41
2.4	Synthesis	42
2.4.1	Aluminium tris (diammine platinum) octacarboxyphthalocyanine	42
2.4.2	Aluminium bis (diammine platinum) octacarboxyphthalocyanine	43
2.4.3	Aluminium trikis (diaqua platinum) octacarboxyphthalocyanine	44
2.4.4	Aluminium tetrakis (diaqua platinum) octacarboxyphthalocyanine	45
2.4.5	Synthesis of platinum nanoparticles	46
3.	Results and discussion	49

3.1 Synthesis and characterization	50
3.1.1 Synthesis	50
3.1.2 Ultraviolet-visible spectroscopy	55
3.1.3 Powder X-ray diffraction and transmission electron microscopy	65
3.2 Photophysical parameters	70
3.2.1 Fluorescence lifetime and quantum yields	70
3.2.2 Triplet state lifetime and quantum yields	74
3.3 Singlet oxygen	77
4. Conclusion	80
4.1 General conclusion	81
4.2 Future perspective	82
5. References	83

LIST OF ABBREVIATIONS

DBU	1,8-diazabicyclo[4.3.0] undec-7-ene
DMSO	dimethylsulfoxide
DNA	deoxyribonucleic acid
F	fluorescence
FT-IR	Fourier transform infra-red
HOMO	highest occupied molecular orbital
IC	internal conversion
ISC	intersystem crossing
IR	infra-red
LUMO	lowest unoccupied molecular orbital
MPc	metallophthalocyanine
Nd:YAG	neodymium-doped yttrium aluminium garnet
NIR	near infra-red
NMR	nuclear magnetic resonance
NP	nanoparticles
OC	octacarboxy
P	phosphorescence
PBS	phosphate buffered saline solution
Pc	phthalocyanine
PDT	photodynamic therapy
ROS	reactive oxygen species
SEM	scanning electron microscopy

T	triplet state
TCSPC	time-correlated single photon counting
TEM	transmission electron microscopy
TLC	thin-layer chromatography
TRES	time-resolved emission spectra
UV-vis	ultraviolet-visible
VC	vibrational cascade
XRD	X-ray diffraction

LIST OF SYMBOLS

α	non-peripheral position/linear absorption
β	peripheral position/full width at half maximum
Δ	heating/change
ϵ	molar extinction coefficient
n	refractive index
π	double bond/numerical value
τ	lifetime
τ_F	fluorescence lifetime
τ_T	triplet state lifetime
Φ	quantum yield
Φ_F	fluorescence quantum yield
Φ_Δ	singlet oxygen quantum yield
Φ_T	triplet state quantum yield
A/abs	absorbance/absorption
C	concentration
d	mean particle size
F	area under fluorescence emission curve
S_0	singlet ground state
S_1	singlet excited state
t	time
T	transmittance
T_1	triplet excited state
x	

LIST OF SCHEMES

Scheme 1.1: Schematic representation of photosensitisation during photodynamic therapy.	4
Scheme 1.2: Synthesis of phthalocyanine from different precursors.	12
Scheme 1.3: Synthesis of octasubstituted phthalocyanine.	14
Scheme 1.4: Synthesis of octacarboxy phthalocyanine.	15
Scheme 1.5: Photodegradation of MPc via a Diels-Adler [4+2] cycloaddition reaction of MPc with singlet oxygen.	29
Scheme 3.1: Synthesis of aluminium bis and tris (diammineplatinum) octacarboxyphthalocyanine.	51
Scheme 3.2: Synthesis of aluminium trikis and tetrakis (diaaquaplatinum) octacarboxyphthalocynine.	53

LIST OF FIGURES

Figure 1.1 Structures of first generation platinum based anticancer compound 8

Figure 1.2 Structures of second generation platinum based anticancer

compound 8

Figure 1.3: Molecular structure of metallophthalocyanine showing α , β positions and isoindole unit 10

Figure 1.4: Aluminium octacarboxy phthalocyanine 16

Figure 1.5: Ground state absorption spectra of unmetallated (a) and metallated (b) Pc. (unpublished work) 17

Figure 1.6: Electronic transitions taking place in phthalocyanines, showing how Q and B bands arise 18

Figure 1.7: Simplified Jablonski diagram showing the electronic transitions of a molecule from the ground state to the excited state. A = absorption, F = fluorescence, VR = vibrational relaxation, IC = internal conversion, ISC = intersystem crossing, P = phosphorescence, S_1 = first singlet excited state, T_1 = first triplet excited state 19

Figure 1.8: Fluorescence decay curve of ZnPc in DMSO (unpublished work) 23

Figure 1.9: Typical triplet decay curve of ZnPc (unpublished work) 24

Figure 1.10: Jablonski diagram showing energy transfer (ET) from a photosensitiser ($^3\text{MPc}^*$) in an excited triplet state to ground state molecular oxygen ($^3\text{O}_2$) leading to the production of singlet oxygen ($^1\text{O}_2$). Other symbols were defined in Fig 1.7

26

Figure 1.11: Graph showing the degradation of DPBF as a singlet oxygen quencher (unpublished work)

28

Figure 2.1: Schematic diagram showing the experimental set up for laser flash photolysis

38

Figure 2.2 Schematic representation of a singlet oxygen set-up

39

Figure 3.1: SEM-EDS data for $(\text{OH})\text{AlOCPc-3Pt}(\text{NH}_3)_2$ showing the different elements in the conjugate

52

Figure 3.2: Ground state absorbance spectra of aluminium octacarboxy phthalocyanine in DMSO (solid black) and PBS (dotted red)

56

Figure 3.3: Absorption (i), excitation (ii) and emission (iii) spectra of $(\text{OH})\text{AlOCPc}$ in PBS

57

Figure 3.4: Ground state absorption spectra of $(\text{OH})\text{AlOCPc}$ at various concentrations: (i) = 9.22×10^{-6} , (ii) = 9.75×10^{-6} , (iii) = 1.06×10^{-5} , (iv) = 1.18×10^{-5} , and (v) = $1.28 \times 10^{-5} \text{ mol. dm}^{-3}$ in DMSO

59

Figure 3.5: Comparative UV-visible spectra for (a) (OH)AlOCPc (i) (OH)AlOCPc-3Pt(H₂O)₂ (ii) and (OH)AlOCPc-4Pt(H₂O)₂ (iii) in DMSO and (b) (OH)AlOCPc (i) and (OH)AlOCPc-3Pt(H₂O)₂ (ii) in water. Concentration $\sim 1 \times 10^{-5}$ M 60

Figure 3.6: Absorption (i), excitation (ii) and emission (iii) spectra of (a) OHAlOCPc-4Pt(H₂O)₂ in DMSO and (b) OHAlOCPc-3Pt(H₂O)₂ in PBS 61

Figure 3.7: Ground state absorption spectra of (OH)AlOCPc-3Pt(H₂O)₂ at various concentrations: (i) = 9.78×10^{-6} , (ii) = 1.04×10^{-5} , (iii) = 1.11×10^{-5} , (iv) = 1.19×10^{-5} , (v) = 1.29×10^{-5} , (vi) = 1.41×10^{-5} and (v) = 1.46×10^{-5} mol. dm⁻³ in DMSO 62

Figure 3.8: Ground state absorbance spectra of (OH)AlOCPc (solid red), (OH)AlOCPc-2Pt(NH₃)₂ (solid black) and (OH)AlOCPc-3Pt(NH₂)₂ (dotted green) in pH 8.2 63

Figure 3.9: Absorption (i), excitation (ii) and emission (iii) spectra of (a) OHAlOCPc-2Pt(NH₂)₂ in pH 8.2 and (b) OHAlOCPc-3Pt(NH₂)₂ in pH 8.2 64

Figure 3.10: Comparative XRD spectrum for OHAlOCPc (a), (b) Pt nanoparticles and OHAlOCPc-3Pt(H₂O)₂ (c) 66

Figure 3.11: TEM images of platinum nanoparticles (a), OHAlOCPc-3Pt(H₂O)₂ (b) and OHAlOCPc-4Pt(H₂O)₂ (c) 68

Figure 3.12: Comparative XRD spectra for (OH)AlOCPc (a) and (OH)AlOCPc-3Pt(NH₃)₃ (b) 69

Figure 3.13: Typical TCSPC decay curve for (OH)AlOCPc-4Pt(H₂O)₂ in DMSO 73

Figure 3.14: Typical TRES spectrum for OHAlOCPc-4Pt(H₂O)₂ showing deconvoluted emissions peaks in DMSO. (i) unquenched and (ii) quenched fluorescence **73**

Fig. 3.15: A transient differential spectrum and inset: triplet decay curve of OHAlOCPc-3Pt(H₂O)₂DMSO. (excitation wavelength = 692 nm in DMSO) **75**

Figure 3.16: Photodegradation of DPBF in the presence of (OH)AlOCPc-3Pt(H₂O)₂ in DMSO **78**

LIST OF TABLES

Table 1.1: Table of phthalocyanines in clinical trials	6
Table 1.2: Table of the phthalocyanine covalent conjugates found in literature	32
Table 3.1: Table of Elemental composition of the conjugates obtained from SEM-EDS	55
Table 3.2: Ground state absorprtion, flourescence emmission and extitation parameters for (OH)AlOCPc, (OH)AlOCPc-2Pt(NH ₃) ₂ , (OH)AlOCPc-3Pt(NH ₃) ₂ , (OH)AlOCPc-3Pt(H ₂ O) ₂ and (OH)AlOCPc-4Pt(H ₂ O) ₂ in different solvents	58
Table 3.3: Table of triplet state parameters for (OH)AlOCPc and its platinated derivatives	71
Table 3.4: Singlet oxygen quantum yields of (OH)AlOCPc and its derivatives in a variety of solvents	79

CHAPTER ONE

INTRODUCTION

The aim of this thesis is to develop bifunctional agents with possible use in both chemotherapy and photodynamic therapy. The study focuses on phthalocyanines which have been modified with platinum complexes. This method is termed “combination therapy”.

1.1 SOME METHODS USED IN CANCER THERAPY

There are many known ways to kill small tumours such as radiation, surgery, chemotherapy and photodynamic therapy [1]. Mostly these techniques are used in conjunction with others to render a more effective treatment, to decrease the dosages and in turn minimise side effects. Radiation, chemotherapy and photodynamic therapy are briefly discussed below.

In radiation therapy the cancerous cells are bombarded with charged particles or high energy radiation from a radioactive source [1,2]. The radioactive or high energy particles damage the DNA of the cells, killing them [1,2]. The radiation is generally directed to the tumour site and not the whole body. However, drawbacks include secondary cancer formation due to radiation exposure [2,3].

Chemotherapy is the use of cytotoxic drugs, where the drugs can be inorganic, organic or biological compounds [4]. The most commonly used drugs are the platinum complexes as they possess high potency. These platinum complexes can bind to the DNA and disrupt cellular processes which lead to cell death. The

drawback with chemotherapy is the lack of selectivity. This then leads to the administration of large doses of the drug which destroys both normal and cancerous cells [4].

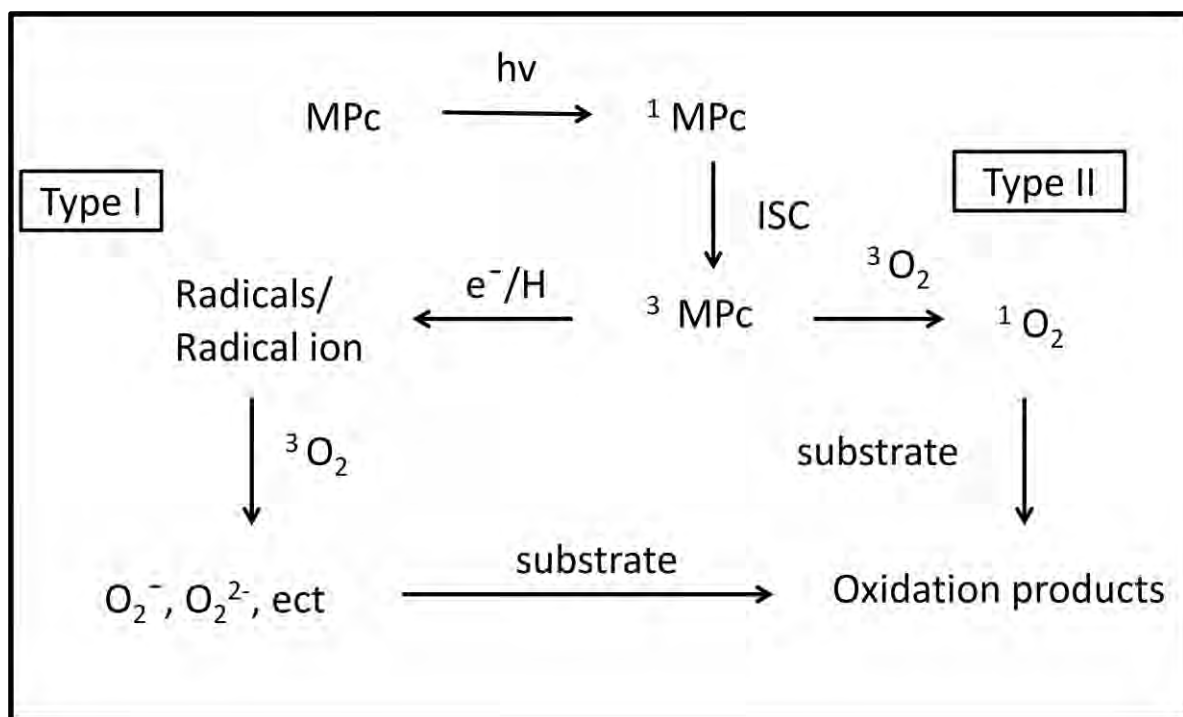
Photodynamic therapy (PDT) is a form of cancer treatment where laser light, molecular oxygen and a photosensitizer (such as a phthalocyanine or porphyrin) are used in combination [5].

1.1.1 MECHANISM OF PHOTODYNAMIC THERAPY

Photodynamic therapy has gained a great deal of attention in the last 30 years as it is a non invasive method for dealing with cancerous cells [5,6]. PDT has been described as having double selectivity in terms of the photosensitiser being retained in tumour cells and the illumination which is localised in the tumour cells [7]. The first generation photosensitisers used in PDT were porphyrins, particularly heamatoporphyrin. It was soon found that porphyrins absorb poorly in the red and near infrared regions, where red light allows for greater tissue penetration [7].

This led to the development of second generation photosensitisers such as phthalocyanines, naphthalocyanines and a variety of chlorins [5,6]. Metallophthalocyanines have displayed superior attributes to their porphyrin counterparts. These attributes include strong absorption in the red region of the spectrum, low toxicity and efficient singlet oxygen production [5]. MPcs also have

the ability to localize selectively in tumour cells and possess notable amounts of fluorescence which can be used tissue imaging. PDT is a treatment dependent on oxygen, and the use of a specific wavelength of light to excite photosensitive dyes. This results in the formation of cytotoxic forms of oxygen (reactive oxygen species) such as singlet oxygen ($^1\text{O}_2$, $^1\Delta_g$), superoxide (O_2^-), peroxide (O_2^{2-}) and hydroxides [8]. These species are generated within cells; they are very reactive and will lead to cell death. The cells that die are the ones within the vicinity of the photosensitiser. The reactive oxygen species (ROS) are produced by one of two mechanisms, namely Type I and Type II (Scheme 1.1). Type I and Type II both stem from the excited triplet state of the photosensitiser.

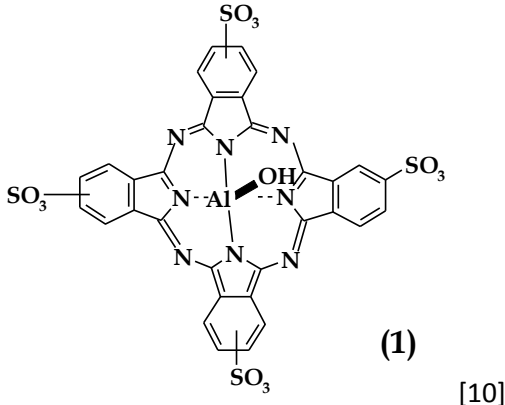
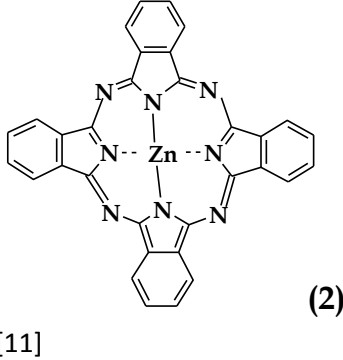
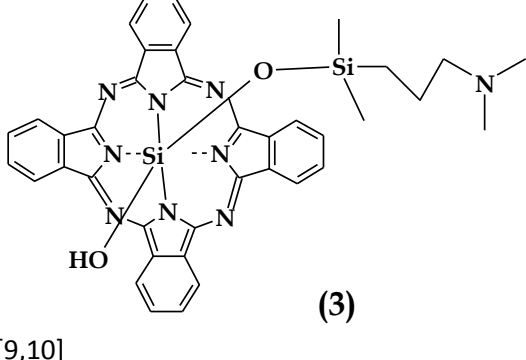


Scheme 1.1: Schematic representation of photosensitisation during photodynamic therapy.

Type I mechanism occurs when the photosensitiser undergoes an electron or hydrogen transfer in its excited state. The electrons and hydrogen interact with molecular oxygen. This process yields radicals, radical ions and ions which are also highly reactive (Scheme 1.1). Direct interaction between the triplet state of the photosensitiser and ground state molecular oxygen is known as the Type II mechanism. The Type II mechanism results in the generation of singlet oxygen, which is a reactive form of molecular oxygen. Most studies suggest that the singlet oxygen (Type II mechanism) is predominant in PDT [5-9].

Phthalocyanines which have made it into clinical trials are listed in Table 1.1 and they include: mixture of differently substituted aluminiumsulfophthalocyanine (**1**, ALPcS_{mix}) [9, 10] which contains a mixture differently sulfonated Pcs, zinc phthalocyanine (ZnPc) (**2**) [11] and Silicon phthalocyanine (Pc 4) (**3**) [9, 10].

Table 1.1: Table of phthalocyanines in clinical trials

Phthalocyanine	Φ_{Δ}	Φ_T	Φ_F	Solvent	Structure
AlPcS _{mix}	0.34	0.44	0.34	PBS	
ZnPc	0.67	0.65 [8]	0.2	DMSO	
SiPc	0.5			DMF	

Φ_{Δ} = singlet oxygen quantum yield, Φ_T = triple state quantum yield, Φ_F = fluorescence quantum yield, DMF = N,N-dimethylformamide, DMSO = dimethyl sulfoxide, PBS = phosphate buffered saline solution.

A short coming of non-water soluble phthalocyanines is in the administration. Thus Pc 4 and ZnPc (which are not water soluble) are solubilised in a complex solvent mixture. This allows the Pcs to be administered into the blood stream. The $\text{AlPcS}_{\text{mix}}$ is water soluble and aggregation is expected to be minimal once in the body [9, 10]. ZnPc and Pc 4 have high singlet oxygen quantum yields in solvents such as: dimethylsulfoxide (DMSO) and *N,N*-dimethylformamide (DMF). The singlet oxygen quantum yields of these two Pcs are misleading because the body uses aqueous media as a solvent.

1.1.2 CHEMOTHERAPY BASED ON PLATINUM DRUGS

The first generation of platinum compound used in cancer therapy was dichloro-diammine-platinum (cis-platin®) (Fig 1.1). It was first used in clinical trials in 1971, and made available to patients in 1978 [4]. However, although it was very potent in killing tumour cells, it had many side effects and was found to be poisonous to normal cells too. Side effects included hair loss and organ toxicity and lowered renal function [12]. It was found that some patients acquired resistance to cis-platin which then led to the development of second generation platinum complexes for cancer treatment. The first generation anti- cancer complexes had a general formula of L_2PtX_2 (Fig 1.1) [13]. X represents labile (good leaving group) ligands such as the halides, hydroxides and carboxylates, while L represents the non labile (non leaving group) ligands such as amines, cyanides and carbonyl groups.

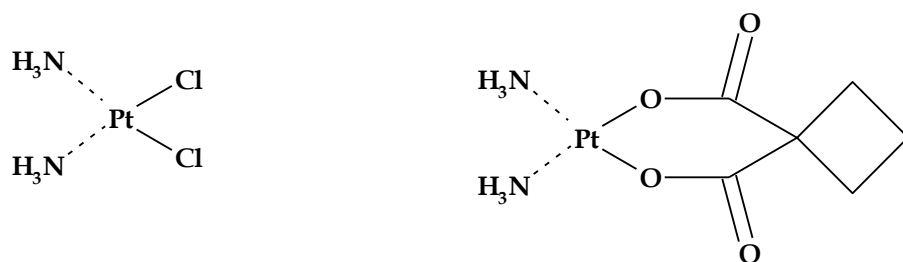


Figure 1.1 Structures of generation platinum based anticancer compound

The second generation compounds on the other hand, do not necessarily follow the same formula (Fig 1.2). The mechanism of action proposed was that the labile ligands provide binding sites for DNA. The platinum ions also bind enzymes which are essential for cellular activity, thus killing cells as all cellular activity ceases

[12,13].

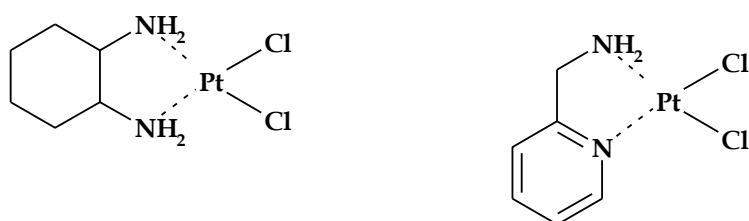


Figure 1.2 Structures of second generation platinum based anticancer compound.

1.2 CHEMISTRY OF PHTHALOCYANINES

1.2.1 HISTORY AND STRUCTURE OF PHTHALOCYANINE

Phthalocyanines (Pcs) have gained significant attention in research since their accidental discovery in 1907 by A. Braun and J. Tcherniac [14]. Braun and Tcherniac discovered a bluish by-product in the synthesis of o-cyanobenzene from phthalimide. The unknown blue compound was found to be insoluble in water and was later identified as a metal free phthalocyanine. Twenty years later, the first metallated phthalocyanine was prepared [15].

In 1934 Linstead coined the term 'phthalocyanine' the *phthalo* part was related to its structural origin from phthalic acid and *cyanine* due to its deep blue colour [15]. Linstead and co-workers prepared a series of metallated phthalocyanines such as iron, copper, magnesium and nickel Pcs [16,17]. Structural elucidation of the Pc was done by J. M Robertson using X-ray diffraction (XRD) [18, 19]. He showed that the unmetalled phthalocyanines were planar compounds, with a chemical formula of $C_{32}H_{18}N_8$ [18, 19].

Phthalocyanines are highly conjugated, planar, macrocyclic, symmetrical molecules. The molecule consists of four isoindole units which are linked together by four nitrogen atoms. The Pc molecule has a two-dimensional 18π electron conjugated system. Approximately 70 metals and non metals have been incorporated into the centre (Fig 1.3) [20]. The chemical and thermal stability of the phthalocyanines is a result of the 18π electron system.

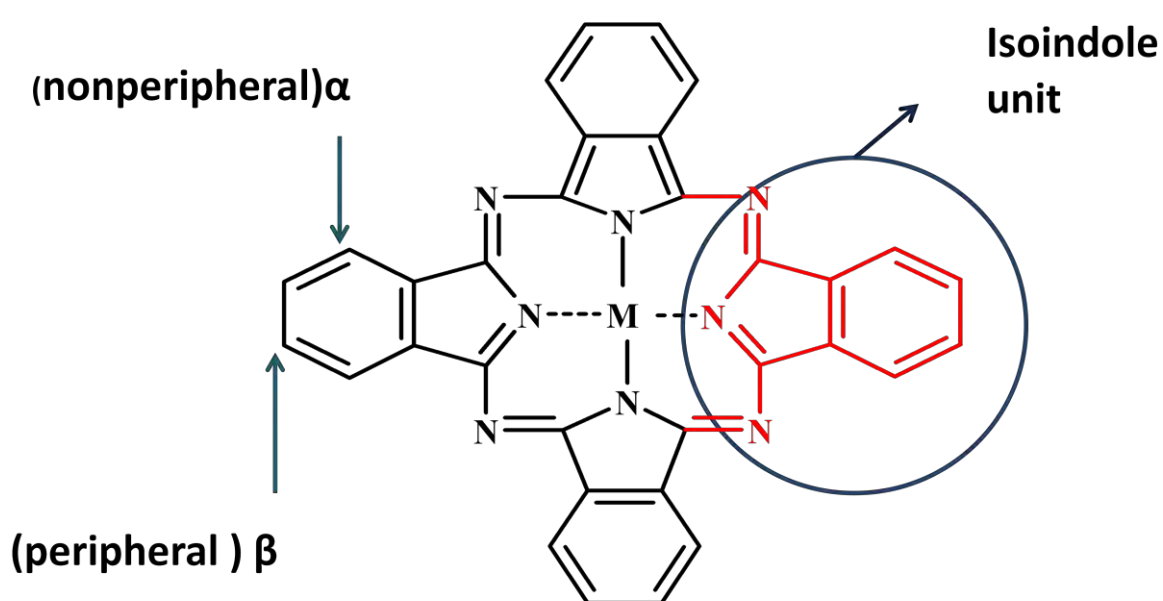


Figure 1.3: Molecular structure of metallophthalocyanine showing α , β positions and isoindole unit.

The extended conjugation provided by the π electron system is responsible for their blue-green colour. The phthalocyanine complexes can be designed for many applications since it has 16 available sites. Substituents can also be introduced to

enhance solubility. Substitutions can be made on the peripheral (β) or non peripheral positions [20, 21].

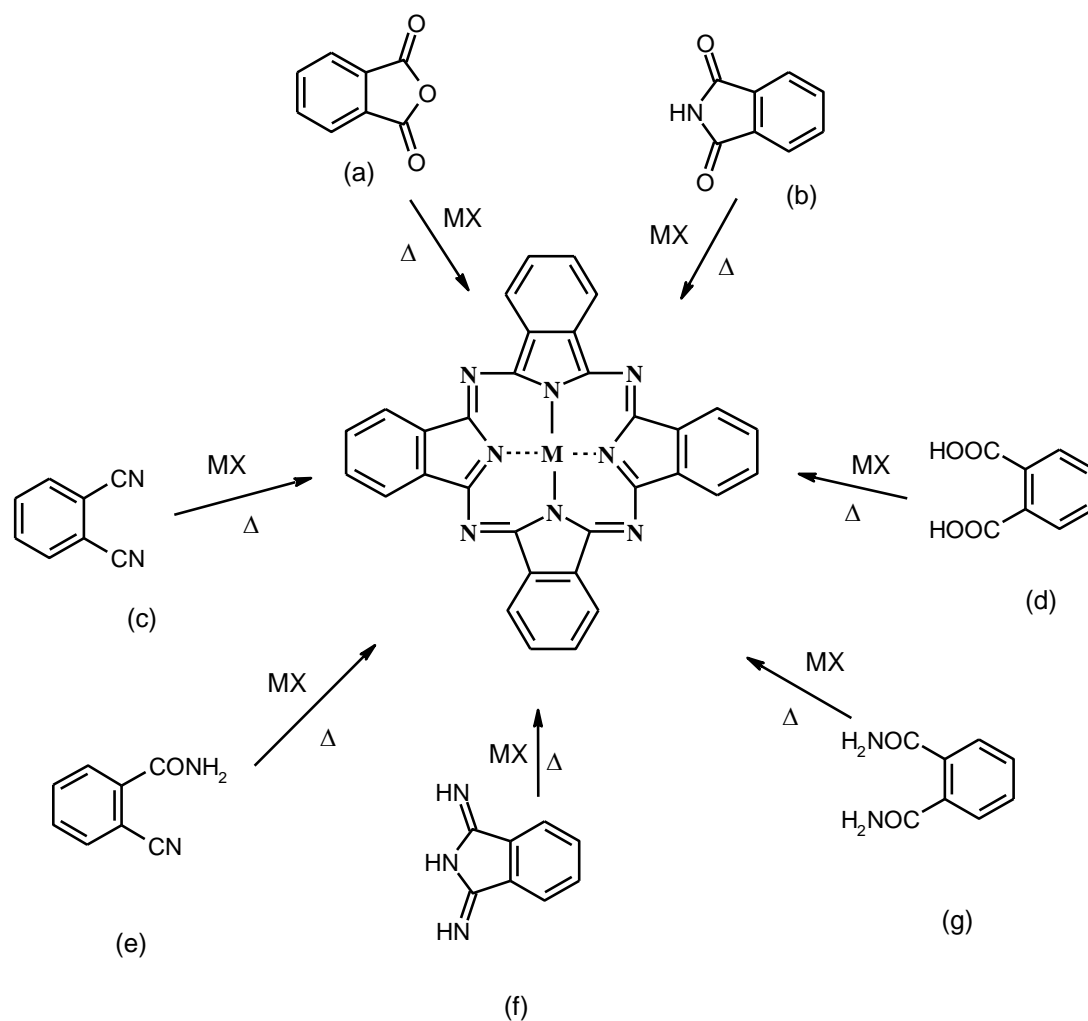
The first application of phthalocyanines was as dyes and pigments in the textile, paint and printing industries [22]. Due to their chemical and thermal stability, low toxicity and low solubility, phthalocyanines have been applied in high technological applications. These applications include use in data storage devices such as recordable compact discs (CD-R) [23], electronics, molecular electronics, semi conductors and photonics [24-26] in electrocatalysts in electrochemical sensor development [27]. Phthalocyanines have recently found applications in, dye sensitised solar cells or photovoltaics [28], non linear optics [22, 29] and in medicine as photosensitisers in photodynamic therapy [6].

1.2.2 PHTHALOCYANINE SYNTHESIS

1.2.2.1 Symmetrical phthalocyanines

A general synthesis for phthalocyanines is the cyclotetramerization reactions (Scheme 1.2) of phthalic acid based precursors, a metal salt and base catalyst. The precursors used include phthalic anhydride (a) [30], phthalimide (b) [30], phthalonitrile (1, 2-dicyanobenzene) (c) [17], phthalic acid (d) [31], o-cyanobenzamide (e) [32], 1,3-diiminoisoindolines (f) and phthalamides (g)[33]. The

success of the synthesis is depended on factors such as precursors, metal salts, solvent, temperature and catalyst. The use of phthalonitrile (c) as a precursor is considered to produce larger yields and products of higherpurity.

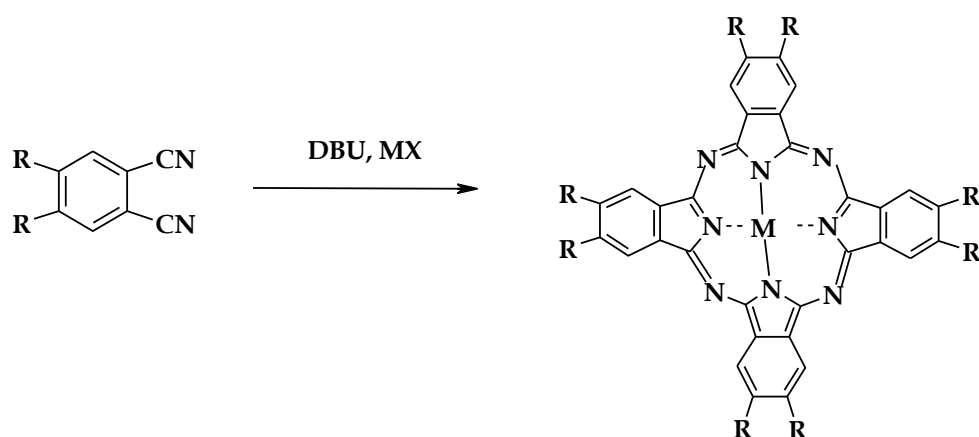


Scheme 1.2: Synthesis of phthalocyanine from different precursors

1.2.2.2 Synthesis of symmetrically octasubstituted phthalocyanine

Unsubstituted phthalocyanines have poor solubility in most organic solvents due to the strong intermolecular interactions taking place between the π -systems, favouring the formation of a strong crystal lattice [34]. The introduction of substituents onto the phthalocyanine ring improves the solubility, because the substituents bring about disorder to the crystal lattice [34, 35].

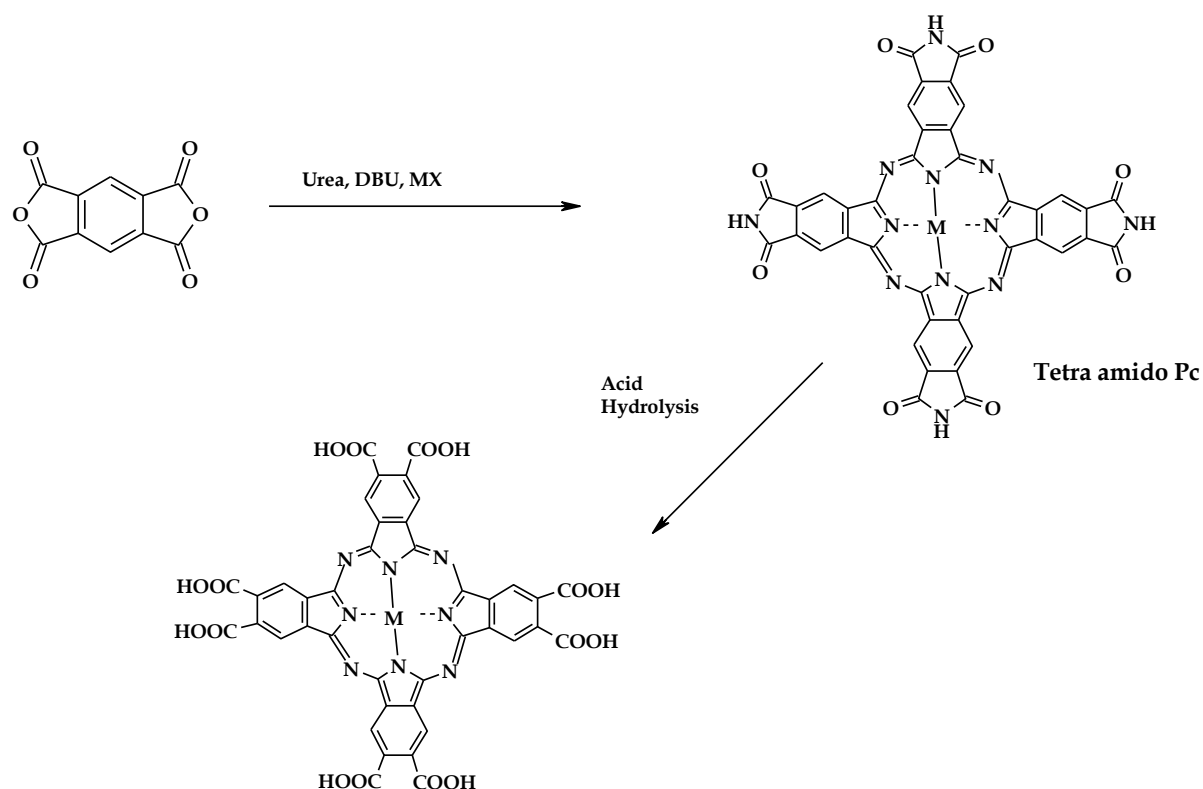
Octasubstituted phthalocyanine are generally synthesised from disubstituted precursors. The substituents are found at positions 4 and 5 (Scheme 1.3) of the phthalonitrile for the production of peripherally substituted phthalocyanines. The 4,5-disubstituted phthalonitriles (Scheme 1.3) are often cyclised at temperatures above their melting point in the presence of a metal salt, a catalyst and basic solvents such as quinoline or aliphatic alcohols. Catalysts such as ammonium molybdate and 1,8-diazabicyclo[4.3.0]undec-7-ene (DBU) are widely employed.



Scheme 1.3: Synthesis of octasubstituted phthalocyanine

1.2.2.3 Synthesis of octacarboxy phthalocyanine

Octacarboxy phthalocyanines (Scheme 1.4) are generally synthesized from the following precursors: benzene-1,2,4, 5-tetracarboxylic acid dianhydride (pyromellitic dianhydride), urea (as a source of nitrogen and solvent), metal salt and 1, 8-diazabicyclo [4.3.0] undec-7-ene (DBU) (catalyst) [36]. The reaction proceeds via a tetra-amido metallophthalocyanine that is formed as an intermediate. The amido groups can then be hydrolysed to the carboxylic acid groups to form octacarboxy phthalocyanine.



Scheme 1.4: Synthesis of octacarboxy phthalocyanine.

1.2.2.4 Phthalocyanine used in this work

In this thesis, aluminium octacarboxy phthalocyanine was used (Fig 1.4). It was selected since it is not aggregated in aqueous media, and the carboxylic acid groups are useful in forming platinum complex conjugates. The conjugation occurs via the negatively charged carboxylate groups which covalently bond to positively charged platinum complexes [37, 38].

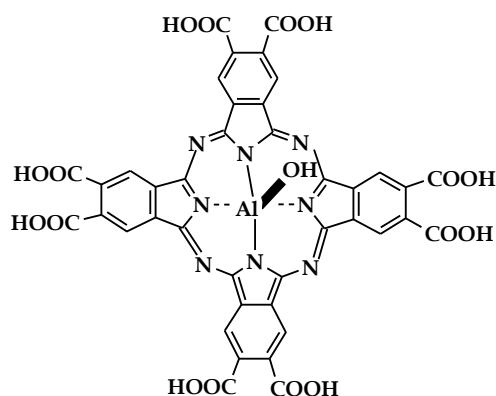


Figure 1.4: Aluminium octacarboxy phthalocyanine

1.2.3 ABSORPTION SPECTRA OF PHTHALOCYANINES

Phthalocyanines can be either metallated or metal free. The metal free phthalocyanine (H_2Pc) is of D_{2h} symmetry. When a metal is incorporated into the phthalocyanine cavity, the symmetry of the phthalocyanine increases from D_{2h} to D_{4h} . The increase in symmetry results in the reduction of allowed electronic transitions.

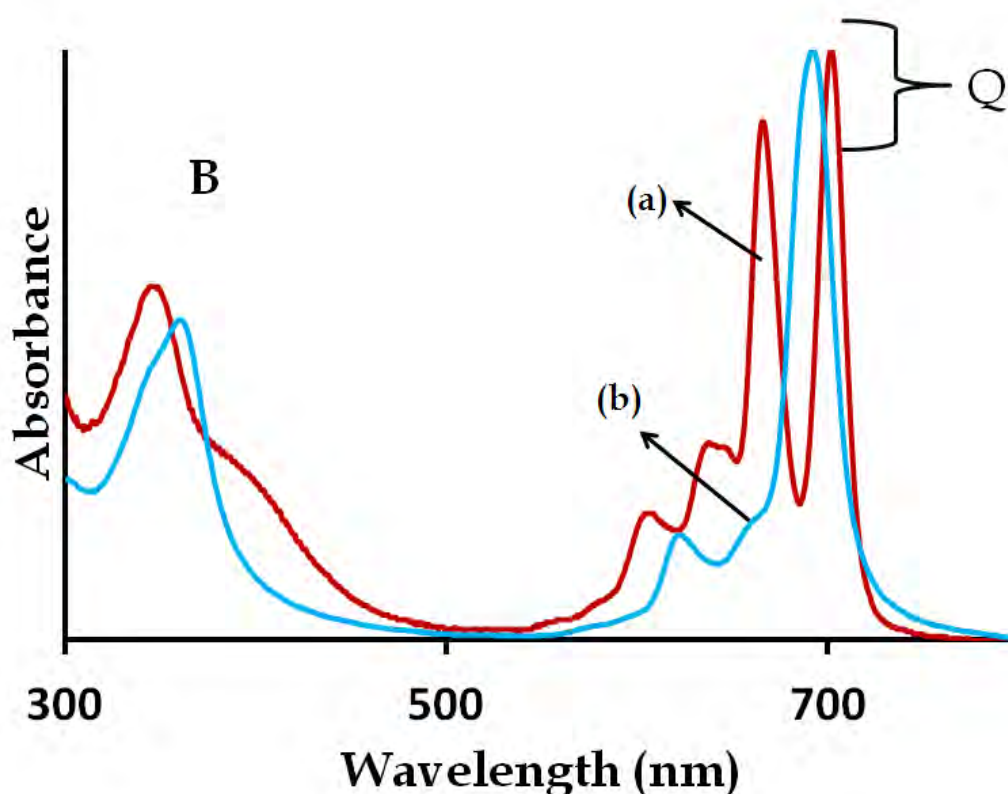


Figure 1.5: Ground state absorption spectra of unmetallated (a) and metallated (b) Pc. (unpublished work)

Metallophthalocyanine spectra are characterised by two main distinct absorption bands, namely the Q-band (~ 670 nm), which is a strong absorption band, and a weaker absorption band called the B band (Fig 1.5) [39]. The bands arise from $\pi - \pi^*$ transitions within the delocalised 18 π electron system of the ring [39, 40]. The bands can be explained in terms of the linear combination of transitions from a_{1u} and a_{2u} , the highest occupied molecular orbitals (HOMO) of the MPc ring to the lowest unoccupied molecular orbitals (LUMO), e.g. The lack of symmetry of an unmetallated

Pc, (H_2Pc) is due to two protons in the central cavity of the Pc ring, which causes the e_g orbitals to lose their degeneracy (Fig 1.6). This results in two allowed electronic transitions with different energies which give rise to a split Q band.

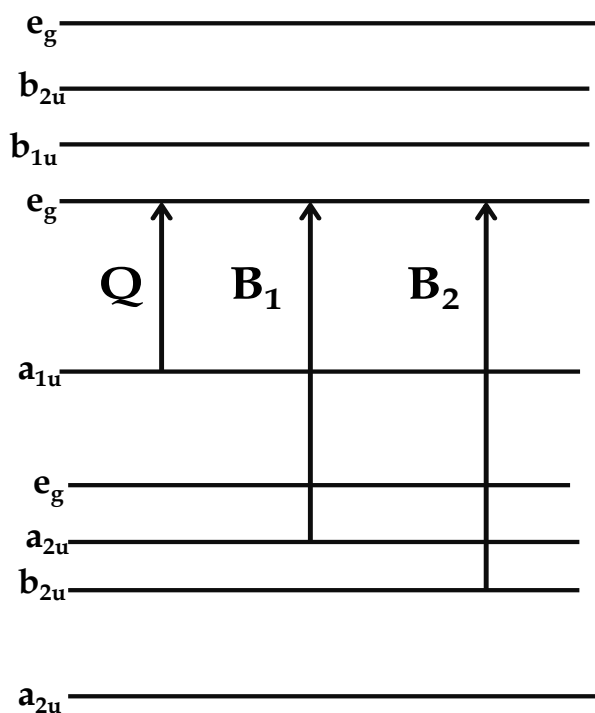


Figure 1.6: Electronic transitions taking place in phthalocyanines, showing how Q and B bands arise.

There are other 3 characteristic bands which phthalocyanines possess in the UV region, namely the N, L, and C bands. They are found in wavelengths below 300 nm and are also due to $\pi - \pi^*$ transitions [40] and are observed only in transparent solvents.

1.2.4 PHOTOPHYSICAL AND PHOTOCHEMICAL PARAMETERS

1.2.4.1 Photophysical parameters

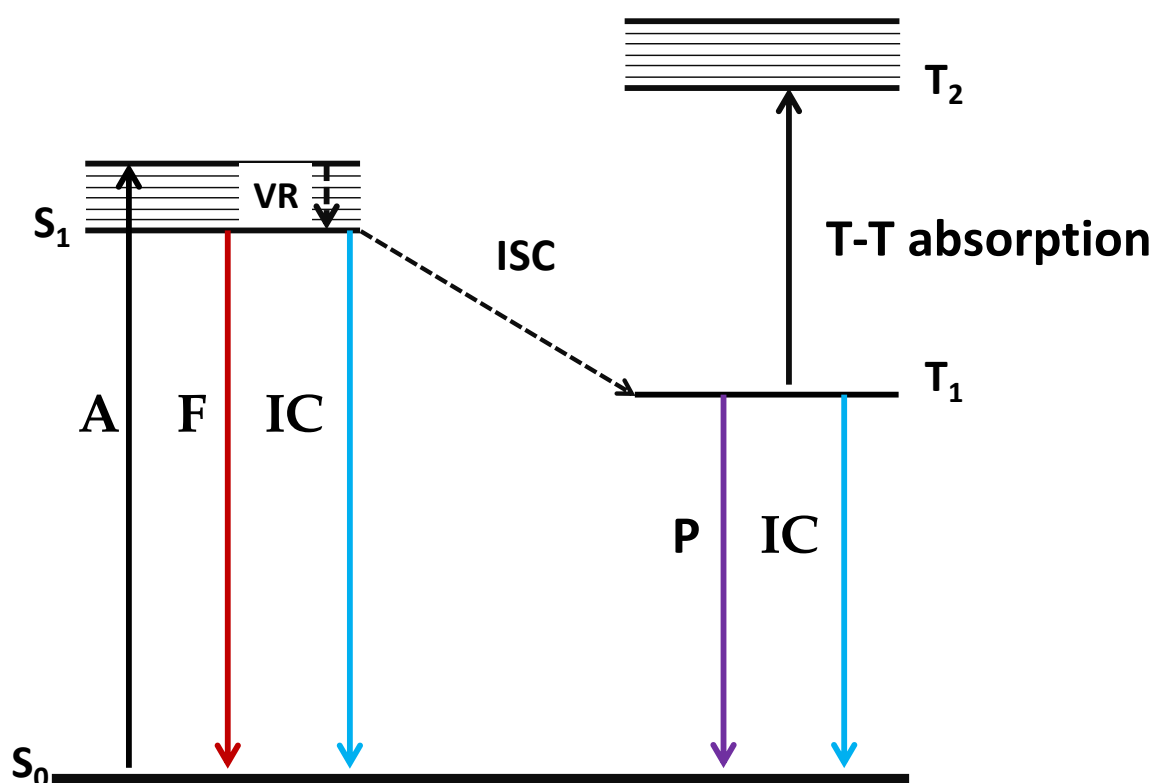


Figure 1.7: Simplified Jablonski diagram showing the electronic transitions of a molecule from the ground state to the excited state. A = absorption , F= fluorescence, VR = vibrational relaxation, IC= internal conversion, ISC = intersystem crossing, P = phosphorescence, S_1 = first singlet excited state, T_1 = first triplet excited state.

Photochemistry is the study of the chemical changes that occur when light interacts with molecules or matter. The net physical processes that occur as a result of interaction are defined as photophysics. It is important to study the photophysical properties of Pcs as this has a direct bearing on their PDT efficiency. The photophysical and photochemical behaviour of a phthalocyanine can be explained by means of a Jablonski diagram (Fig 1.7) [41]. When a molecule absorbs light (**A**), it is excited from the ground state (S_0) to the vibronic levels of the first excited singlet state (S_1). The molecule may then lose some of its energy, due to the collisions taking place in a process called vibrational relaxation (**VR**), to the lowest vibronic levels of the first excited state (S_1). The vibrational relaxation is frequently found in molecules in solution or in a condensed phase. The molecule can return to its ground state (S_0), by a radiative process called fluorescence (**F**) or by a non-radiative process called internal conversion (**IC**), where the energy is released as heat to its surroundings. The other possibility is that the molecule can undergo intersystem crossing (**ISC**) to the first excited triplet state (T_1).

The process of intersystem crossing is a change in multiplicity, which is a spin-forbidden process according to quantum mechanical selection rules. Even though **ISC** is a spin-forbidden process it still occurs due to spin orbit coupling which causes the 'mixing' of the singlet and triplet states by making them isoenergetic [41]. Heavy atoms have large spin orbit coupling which therefore encourage **ISC**. The energy from the first excited triplet state (T_1) may be lost by internal (**IC**) or by emission of

light through phosphorescence (**P**). In the presence of molecular oxygen, which is in its ground state, the photosensitizer may transfer its energy to ground state oxygen to produce singlet oxygen by photosensitization.

1.2.4.2 Fluorescence quantum yields and lifetimes

The amount of fluorescence emission from the singlet state is quantified by the fluorescence quantum yield (Φ_F), which measures the efficiency of the fluorescence process. Quantum yields are defined as the number of photons taking part in an event for every photon absorbed. Therefore the fluorescence quantum yield (Φ_F) is defined by the number of molecules fluorescing per number of photons absorbed. The fluorescence quantum yield is determined by a comparative method [42,43] using a compound that has a known Φ_F (i.e. a standard). In this thesis ZnPc is used, where ZnPc in DMSO (Φ_F) = 0.20 [44], and Equation 1.1 was employed.

$$\Phi_F = \Phi_{F(\text{std})} \frac{F \cdot A_{\text{std}} n^2}{F_{\text{std}} \cdot A n^2} \quad (1.1)$$

where F and F_{std} are the areas under the fluorescence curves of the sample and standard, respectively. A and A_{std} are the absorbances of the sample and standard,

respectively, at the excitation wavelengths, and n and n_{std} are the refractive indices of the solvents used for the sample and standard. Very low concentrations are used for the Φ_F determination to avoid self quenching. The factors that affect the fluorescence properties are temperature, solvent type, aggregation and metal ions present. The solvent effects include polarity, viscosity and refractive index. These factors affect the fluorescence intensity, fluorescence quantum yield [44] and fluorescence lifetime (τ_F). The fluorescence lifetime can be determined using a number of techniques [45, 46], with time domain measurements being more commonly used [46]. The equipment used for time-domain is based on gating the fluorescence signal using a time-correlated single-photon counting (TCSPC) [47]. A typical fluorescence decay curve is shown in (Fig 1.8). The fluorescence lifetime can also be determined using the absorbance and emission spectra of MPcs using the Strickler-Berg equation.

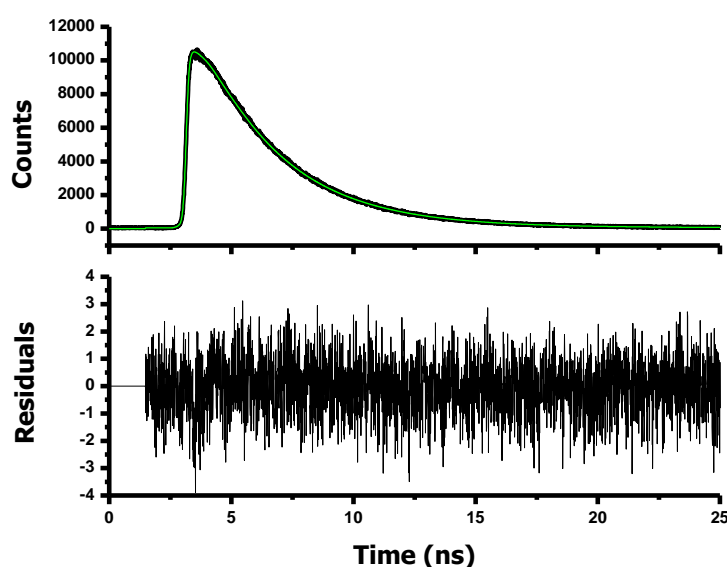


Figure 1.8: Fluorescence decay curve of ZnPc in DMSO (unpublished work)

The fluorescence lifetimes of phthalocyanines generally range in the order of a few nanoseconds.

1.2.4.3. Triplet quantum yields and lifetimes

Laser flash photolysis is a technique used to measure triplet absorbance and this is directly related to the triplet quantum yields of photosensitisers [50].

The triplet state parameters determined include the triplet quantum yields (Φ_T) and triplet lifetimes (τ_T). The triplet lifetimes are determined from the triplet decay curve (Fig 1.9) using the OriginPro 8 software.

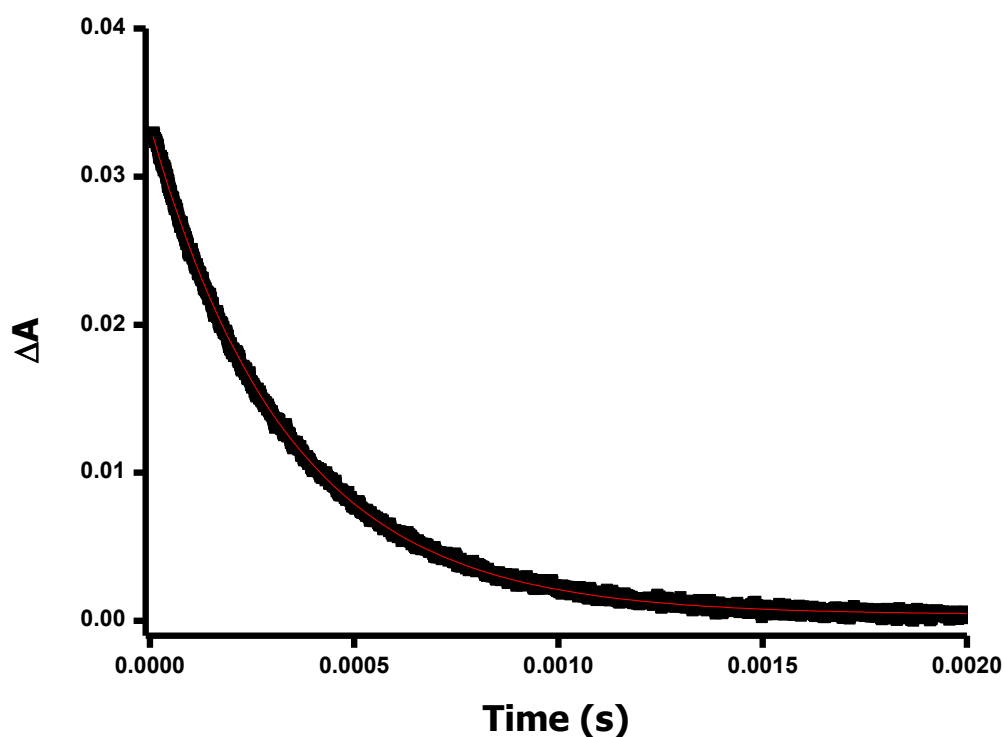


Figure 1.9: Typical triplet decay curve of ZnPc (unpublished work).

The triplet quantum yield (Φ_T) is used to determine the efficiency of the triplet state of the phthalocyanine as a photosensitizer and is also used to quantify the molecules in the triplet state. The phthalocyanines usually have triplet absorption spectra in the region of ~ 500 nm. The experiment measures the changes in the triplet absorption (ΔA_T) as well changes in the ground singlet state (ΔA_S) which is related to the triplet state quantum yield.

The triplet quantum yields may be determined using a comparative method [50, 51] which is based on the decay of the triplet state using equation 1.2

$$\Phi_T = \Phi_T^{\text{Std}} \frac{\Delta A_T \varepsilon_T^{\text{Std}}}{\Delta A_T^{\text{Std}} \varepsilon_T} \quad (1.2)$$

where ΔA_T and ΔA_T^{Std} are the changes in triplet state absorbances of the sample and the standard, respectively. $\varepsilon_T^{\text{Std}}$ and ε_T are the triplet state extinction coefficients of the standard and sample, respectively. Φ_T^{Std} is the triplet state quantum yield for the standard in this case, ZnPc in DMSO. The ε_T is determined using the change in ground singlet state absorbance (ΔA_S), change in the triplet state (ΔA_T) absorbance and extinction coefficient (ε_S) of the ground state using equations 1.3 a and 1.3 b

$$\varepsilon_T = \varepsilon_S \frac{\Delta A_T}{\Delta A_S} \quad (1.3 \text{ a})$$

$$\varepsilon_T^{\text{Std}} = \varepsilon_S^{\text{Std}} \frac{\Delta A_T^{\text{Std}}}{\Delta A_S^{\text{Std}}} \quad (1.3 \text{ b})$$

The photophysical parameters i.e. triplet quantum yield (Φ_T) and the fluorescence quantum yields (Φ_F), complement each other and should add up to 1, if there is no

energy lost through internal conversion. This means that if the triplet quantum yield (Φ_T) value is high, a corresponding low fluorescence quantum yield (Φ_F) will be obtained and vice versa.

1.2.4.4 Singlet oxygen quantum yield

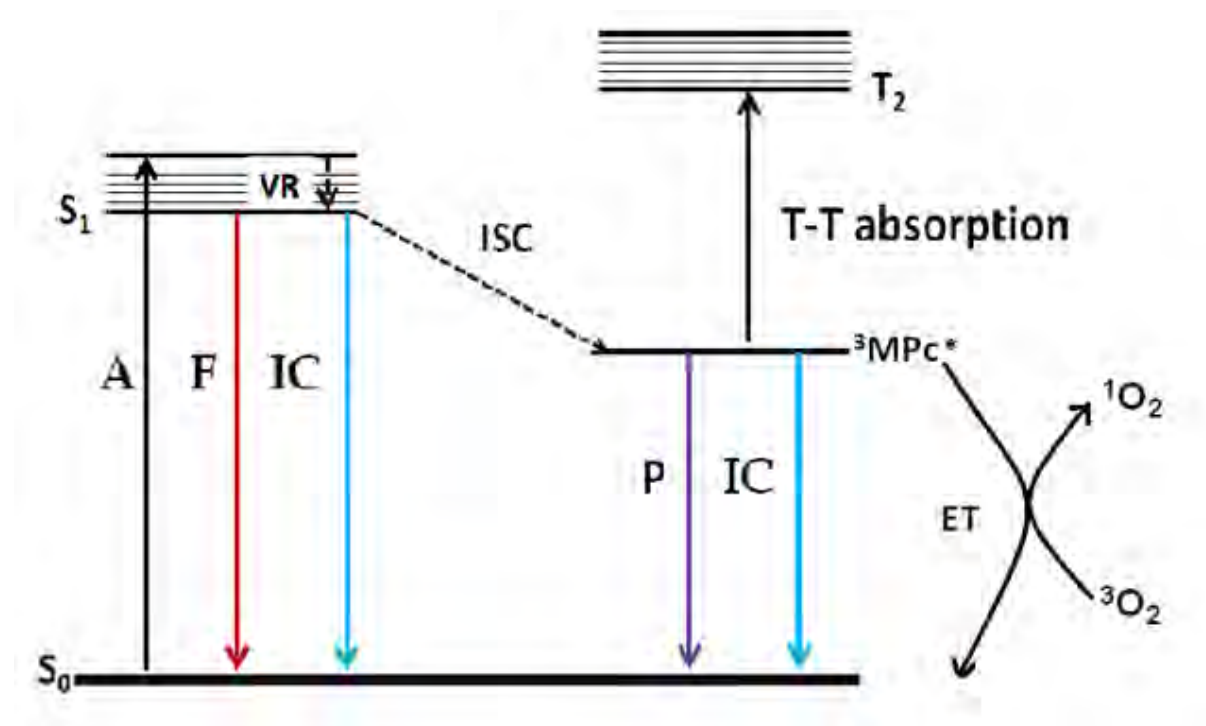


Figure 1.10: Jablonski diagram showing energy transfer (ET) from a photosensitiser ($^3\text{MPC}^*$) in an excited triplet state to ground state molecular oxygen ($^3\text{O}_2$) leading to the production of singlet oxygen ($^1\text{O}_2$). Other symbols were defined in Fig 1.7.

Photosensitization involves the processes shown in Fig 1.10. The excited state phthalocyanine molecule ($^3\text{MPc}^*$) transfers its energy to triplet molecular oxygen ($^3\text{O}_2$).

The energy required for the excitation of ground state molecular oxygen is $\sim 94 \text{ kJ mol}^{-1}$ to form singlet oxygen which is less than the energy that the excited state molecule ($^3\text{MPc}^*$) has ($\sim 110 - 126 \text{ kJ mol}^{-1}$) [52, 53]. The singlet oxygen quantum yield (Φ_{Δ}) can be calculated by equation 1.4:

$$\Phi_{\Delta} = \Phi_{\Delta}^{Std} \frac{RI_{abs}^{Std}}{R^{Std}I_{abs}} \quad 1.4$$

where Φ_{Δ}^{Std} is the singlet oxygen quantum yield of the standard, R^{Std} and R are the singlet oxygen quencher (e.g 1,3-diphenylisobenzofuran (DPBF)) photobleaching rate in the presence of the standard and sample, respectively. I_{abs} and I_{abs}^{Std} are the rates of light absorption for the sample and standard, respectively. In this method, the solution of the sample is mixed with the quencher and irradiated. The singlet oxygen generation is then monitored by the decrease in the absorption maximum (Fig 1.11) [54] of the quencher (eg DPBF at $\sim 416 \text{ nm}$ in DMSO).

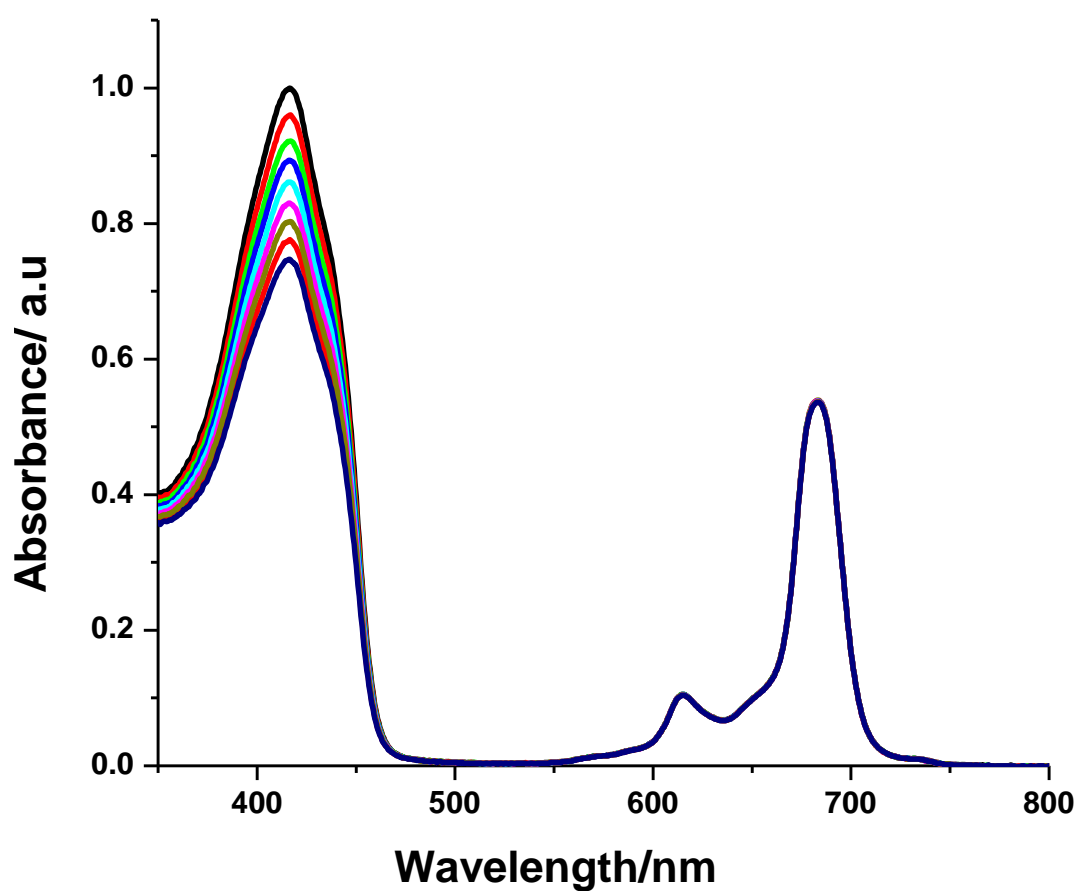
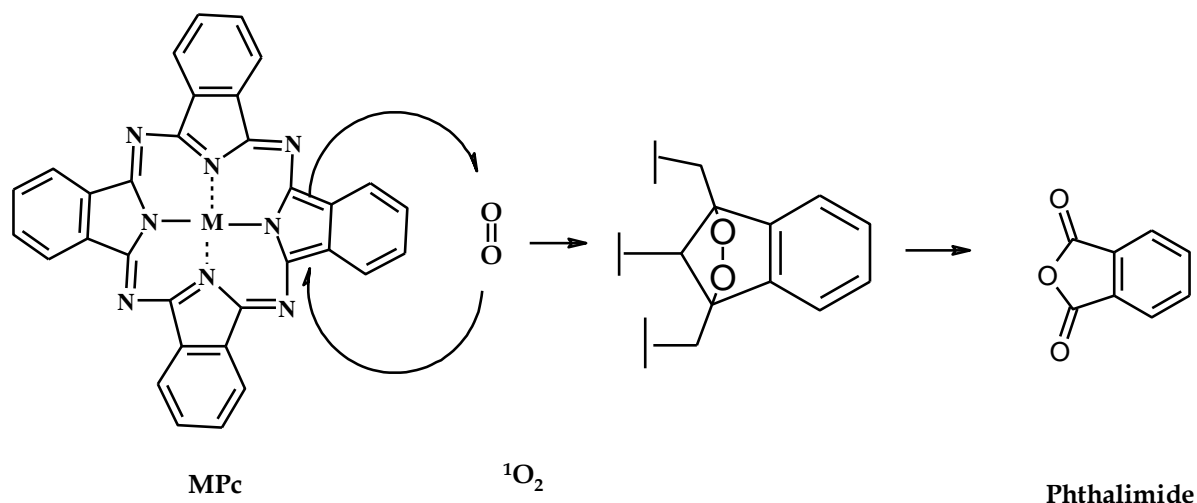


Figure 1.11: Graph showing the degradation of DPBF as a singlet oxygen quencher (unpublished work).

1.2.4.5 Photodegradation/ Photobleaching

Photobleaching is a photochemical process where the phthalocyanine ring is degraded into smaller fragments. The process is driven by singlet oxygen in the presence of light which leads to photo-oxidation products [55].

The mechanism occurs via a Diels-Alder [4+2] cycloaddition reaction where the phthalocyanine acts as a diene and the singlet oxygen as a dienophile, Scheme 1.5 [55].



Scheme1.5: Photodegradation of MPc via a Diels-Adler [4+2] cycloaddition reaction of MPc with singlet oxygen.

There are many factors that can influence the process of photodegradation. The singlet oxygen is an electron poor dienophile and will react readily with a phthalocyanine bearing electron donating substituents. Electron withdrawing groups will stabilize the Pc and hinder the oxidation of the Pc by singlet oxygen [56].

The nature of the solvent employed in the experiment also plays a role in the photodegradation of the Pc. Solvents that are basic such as dimethylsulfoxide (DMSO) coordinate to the metal centre and shield the Pc from oxidative attack. Chlorinated solvents such as dichloromethane (DCM), as a result of their low basicity, promote photodegradation [44, 56, 57]. In the presence of a singlet oxygen quencher, the photodegradation rates are reduced, due to the quencher's ability to react with singlet oxygen. The photodegradation quantum yield (Φ_{PD}) is calculated using equation 1.5 [57]

$$\Phi_{PD} = \frac{(C_0 - C_t)VN_A}{I_{abs}St} \quad (1.5)$$

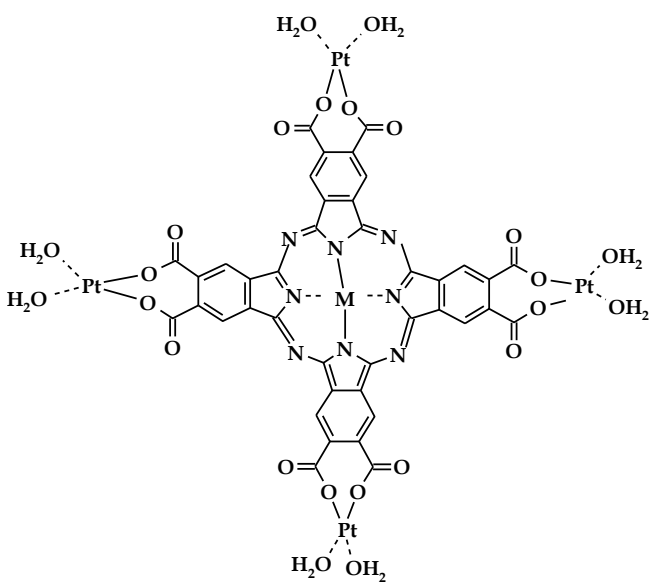
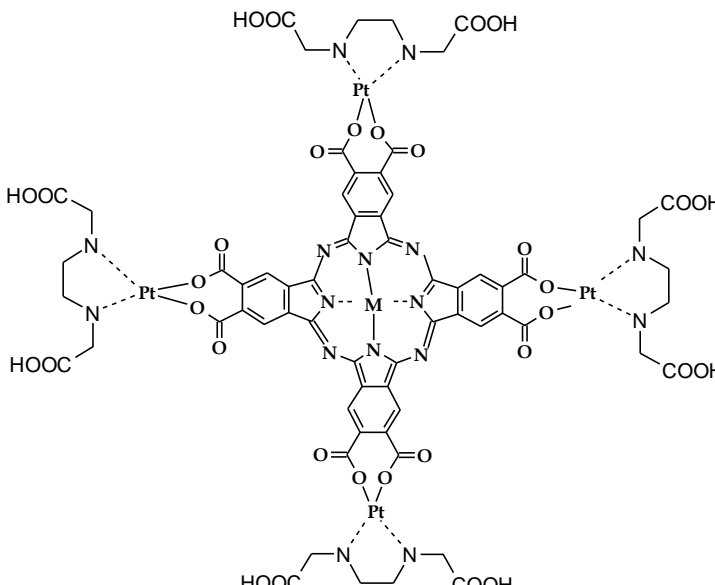
where C_0 and C_t are the concentration of the phthalocyanine before and after irradiation, respectively, V is the reaction volume, N_A the Avogadro's number, I_{abs} is the overlap integral of the radiation source intensity and the absorption of the MPc in the region of the interference filter transmittance [57], S is the irradiated cell area and t is the irradiation time in seconds.

1.3 COVALENT PHTHALOCYANINE PLATINUM CONJUGATE

Dolotova *et al* synthesised the first covalent phthalocyanine platinum conjugates [37]. The phthalocyanine used in the conjugation was an octacarboxy phthalocyanine and methanol and ethanol were used as solvents. In literature the octacarboxy phthalocyanine (OCPC) used had paramagnetic central metal ions (Table 1.2) [37,38, 58,59]. All complexes were tetra substituted with platinum complexes hence they were insoluble in water. Recently, a zinc version was observed in literature with mono, di, tri and tetra platination [60,61]. For ZnOCPC- n Pt(H₂O)₂ complexes mono, di and tri platinated conjugates were water soluble except for the tetra platinated. Most of the phthalocyanine covalent conjugates in literature have the platinum diaqua complex (MOCPc-4Pt(H₂O)₂) and this work introduces the platinum ammine complex (MOCPc- n Pt(NH₃)₂), which is closer to cis-diamminedichloro-platinum (cis-platin®) and is a structurally analogues of cis-diammine(1,1-cyclobutanedicarboxylato)platinum (carboplatin®).

The iron phthalocyanine version of the conjugate was used in the electrocatalytic oxidation of formic acid into carbon dioxide and water, showing that the conjugate can be used to oxidise toxic chemicals into non toxic products. The ruthenium conjugate was shown to have potential use in fuel cells as an electrocatalyst since it showed the total reduction of oxygen into water.

Table 1.2: Table of the phthalocyanine covalent conjugates with platinum found in literature

Conjugate	Metal ion	ref
	Co	37
	Fe	58
	Ru	59
	Zn	60
	Co	38
	Zn	61

In this thesis we explore the use of aluminium octacarboxy phthalocyanine in the synthesis of a conjugate with platinum (II) complexes. Aluminium, as a central metal, was selected since it is highly photoactive. The influence of the platinum complex (as a conjugate) on the photophysical properties of the OHAlOCPc is investigated.

1.3. SUMMARY OF AIMS

The aims of this thesis are summarised as follows:

1. The synthesis and spectroscopic characterization of aluminium octacarboxy phthalocyanine (OHAlOCPc). The conjugation of OHAlOCPc with the cis-dichloro-diammineplatinum and potassium tetra chloroplatinate.
2. To investigate and compare the photophysicochemical behaviour such as: fluorescence quantum yields, triplet quantum yields and lifetimes, singlet oxygen quantum yields for MOCPc and the conjugates.

CHAPTER TWO

EXPERIMENTAL

2.1 MATERIALS

For synthesis and characterization: 1,8-Diazobicyclo[5.4.0] undec-7-ene (DBU), oleic acid, pyromellitic dianhydride, and platinum acetylacetonate ($\text{Pt}(\text{acac})_2$) were purchased from Fluka, while *cis*-diamminedichloroplatinum, 1,2-dicyanobenzene, and silver nitrate were purchased from Aldrich. Methanol (MeOH), aluminium chloride, ethanol (EtOH) and sodium hydroxide were purchased from Saarchem. Potassium hexachloroplatinate pyromellitic dianhydride, diphenyl ether, oleylamine, 1,2-hexadecanediol and ZnPc were also purchased from Aldrich. AlPc was synthesised according to modified literature method [17]. AlPcSmix was synthesised by literature method [62]

Photophysicochemistry: 1,3-diphenylisobenzofuran (DPBF) and 9,10-anthracenediyl-bis(methylene)dimalonic acid (ADMA) were purchased from Aldrich.

Solvents: Sulfuric acid (98 %), nitric acid (55 %), hydrochloric acid (32%), quinoline, acetone, 2-propanol, dimethylsulfoxide (DMSO) were SAARChem. Uvasol® DMSO (spectroscopic grade) was purchased from Merck.

2.2 EQUIPMENT and INSTRUMENTAL

1. Column chromatography was performed on aluminium oxide 90 (0.04 – 0.200 mm) and preparative thin layer chromatography was performed on aluminium oxide 60 F₂₅₄.
2. The ultra violet –visible (UV-Vis) were recorded on a Shimadzu UV 2550 UV-Vis/NIR spectrophotometer.
3. IR spectra (KBr pellets and nujol) were recorded on a on a Perkin–Elmer Spectrum 100 ATR FT-IR and Perkin–Elmer Spectrum 400FT-IRspectrometers.
4. Fluorescence excitation and emission spectra were recorded on a Varian Eclipse spectroflourimeter.
5. Elemental analyses were carried out on a Vario EL III MicroCube CHNS Analyzer.
6. Mass spectral data were collected with a Bruker AutoFLEX III Smartbeam TOF/TOF Mass spectrometer. The instrument was operated in positive ion mode using a mass range of 400-3000 amu. The voltage of the ion sources were set at 19 and 16.7 kV for ion sources 1 and 2 respectively, while the lens was set at 8.50 kV. The reflector 1 and 2 voltages were set at 21 and 9.7 kV respectively. The spectra were acquired using dithranol as the MALDI matrix, using a 354 nm nitrogen laser as the ionising source.

7. Transmission electron microscope (TEM) images were recorded using JEOL JEM 1210 at 100 kV accelerating voltage.
8. Scanning electron microscope (SEM) images were recorded using VAGA TESCAM at 20 kV accelerating voltage. Energy dispersive spectroscopy (EDS) was done on a INCA PENTA FET coupled to the VAGA TESCAM using 20 kV accelerating voltage.
9. Fluorescence lifetimes and time resolved spectroscopy (TRES) were measured using a time correlated single photon counting (TCSPC) setup (FluoTime 200, Picoquant GmbH) with a diode laser (LDH-P-670 with PDL 800-B, Picoquant GmbH, 670 nm, 20 MHz repetition rate, 44 ps pulse width). Fluorescence was detected under the magic angle with a Peltier cooled photomultiplier tube (PMT) (PMA-C 192-N-M, Picoquant) and integrated electronics (PicoHarp 300E, Picoquant GmbH). A monochromator with a spectral width of about 8 nm was used to select the required emission wavelength band. The response function of the system, which was measured with a scattering Ludox solution (DuPont), had a full width at half-maximum (FWHM) of 300 ps. All luminescence decay curves were measured at the maximum of the emission peak and lifetimes were obtained by deconvolution of the decay curves using the FluoFit Software program (PicoQuant GmbH, Germany). The support plane approach [63] was used to estimate the errors of the decay times.
10. X-ray powder diffraction (XRD) patterns were recorded on a Bruker D8 Discover equipped with a Lynx eye detector, using Cu-K α radiation (1.5405 Å,

nickel filter). Data were collected in the range from $2\theta = 5^\circ$ to 100° , scanning at 1° min^{-1} with a filter time-constant of 2.5 s per step and a slit width of 6.0 mm. Samples were placed on a silicon wafer slide. The X-ray diffraction data were treated using Eva (evaluation curve fitting) software. Baseline correction was performed on each diffraction pattern.

11. A laser flash photolysis (Fig. 2.1) system was used to determine the triplet quantum yields and lifetimes. The excitation pulses were produced by a Quanta-Ray Nd:YAG laser (1.5 J/9 ns), pumping a Lambda Physik FL 3002 dye laser (Pyridin 1 in methanol). The analysing beam source was from a Thermo Oriel xenon arc lamp and a photomultiplier tube was used as a detector. The signals were recorded with a two channel 300 MHz digital oscilloscope (Tektronix TDS 3032C).

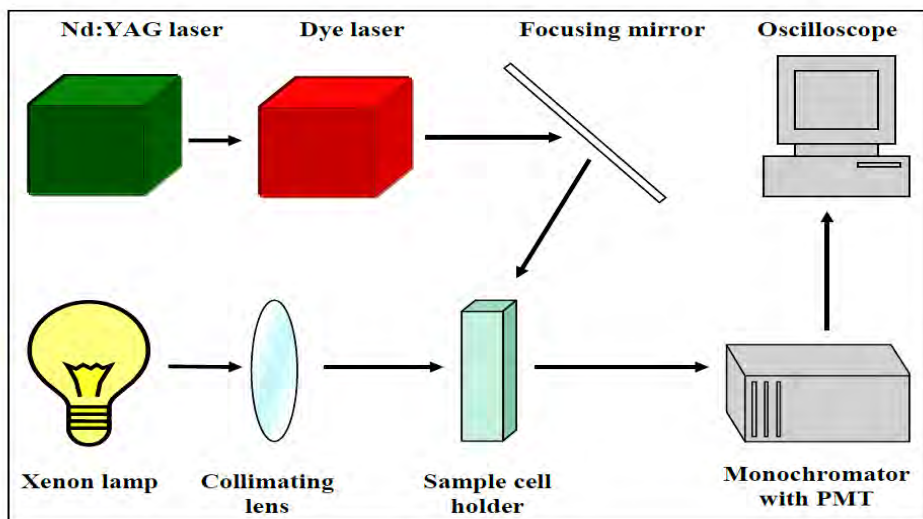


Figure 2.1: Schematic diagram showing the experimental set up for laser flash photolysis.

12. Photo-irradiations (Fig. 2.2) for singlet oxygen studies were done using a General Electric Quartz line lamp (300W). A 600 nm glass cut off filter (Schott) and a water filter were used to filter off ultraviolet and infrared radiations respectively. An interference filter (Intor, 700 nm with a band width of 40 nm) was additionally placed in the light path before the sample. Light intensities were measured with a POWER MAX5100 (Molelectron detector incorporated) power meter. A light intensity of 2.15×10^{16} photons $\text{s}^{-1} \text{cm}^{-2}$ was employed for Φ_{Δ} determinations.

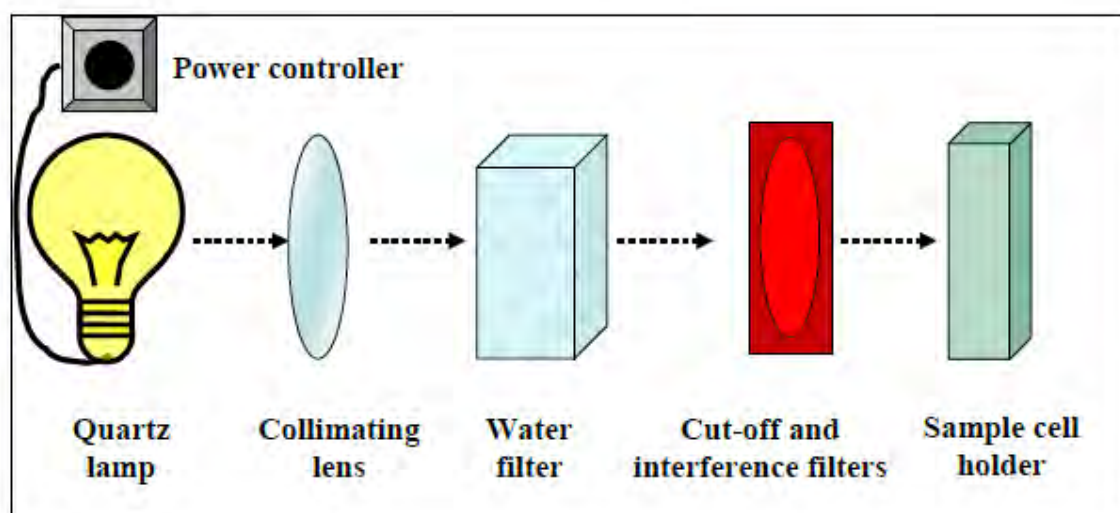


Figure 2.2 Schematic representation of a singlet oxygen set-up.

2.3 METHODS

2.3.1 Fluorescence and triplet quantum yields and lifetimes

Fluorescence quantum yield were determined using Equation 1.1, using unsubstituted ZnPc in DMSO ($\Phi_F = 0.2$) as a standard [44]. For each study at least two independent experiments were performed for quantum yield determinations. Both the sample and the standard were excited at the same relevant wavelength.

For the laser flash photolysis experiments, the MPc solution ($A \sim 1.5$) was bubbled with argon for 30 minutes in a 1 cm path-length spectrophotometric cell and irradiated at the Q-band using the laser flash photolysis. Triplet quantum yields (Φ_T) were calculated using Equation 1.2. Unsubstituted ZnPc in DMSO ($\Phi_T = 0.65$) [50] and AlPcSmix (mixture of differently substituted aluminium sulfophthalocyanine) in aqueous solutions ($\Phi_T = 0.44$) [64] were used as standards. Triplet lifetimes were determined by exponential fitting of the kinetic curves using OriginPro 8 software.

2.3.2 Singlet oxygen

Singlet oxygen quantum yields (Φ_{Δ}) were determined using Equation 1.4. An air-saturated solution of the phthalocyanine under investigation (~ 3.0 mL) containing the singlet oxygen quencher (DPBF or ADMA depending on the sample), was prepared in the dark (Q-band absorbance ~ 0.7 in the final solution). The solution was placed in a 1 cm pathlength spectrophotometric quartz cell and illuminated by using the set up shown in Figure 2.2.

The wavelength of the interference filter was chosen such that it was close to the Q-band absorption of the MPc of interest. The absorbance decay of the singlet oxygen quencher (ADMA at 380 nm in aqueous media and DPBF at 417 nm in DMSO) was monitored with time and used for the calculation of Φ_{Δ} . The concentrations of the quenchers were kept at $\sim 4 \times 10^{-5}$ M to avoid chain reaction and to maintain the highest solubility since the quenchers are partially soluble. ZnPc ($\Phi_{\Delta}^{\text{Std}} = 0.67$) in DMSO [65] and AlPcSmix ($\Phi_{\Delta}^{\text{Std}} = 0.38$) [66] in aqueous solutions, were used as standards in the singlet oxygen quantum yield determination.

2.4. SYNTHESIS

The OHAlOCPc [36] and its sodium salt [67] were synthesised, purified and characterized according to modified method found in literature [36, 67]. The prepared phthalocyanine was covalently coordinated to K_2PtCl_4 and cis-diamminedichloroplatinum.

2.4.1. Hydroxo aluminium *tris* (diammine platinum) octacarboxy phthalocyanine (OHAlOCPc-3Pt(NH₃)₂) (Scheme 3.1)

An aqueous solution of cis-diamminedichloroplatinum (55 mg, 0.19 mmol) and silver nitrate (47 mg, 0.28 mmol) in 10 mL deionised water was stirred in the dark for 24 h [13,38]. This was done to solubilise cis-diamminedichloroplatinum in water. As soon as the two salts were added together, the precipitation of silver chloride occurred. The precipitate was filtered after 24 h of reaction. The filtrate was collected and mixed with a solution of the sodium salt of OHAlOCPc (0.05 g, 0.045 mmol). The ratio of number of moles for Pc: Pt was 1:4. The solution was stirred for 4 h at 55 °C, following literature methods [13,38]. The solution was allowed to stand for 12 h and the precipitate was collected. The conjugate was washed with water, ethanol, acetone and diethyl ether.

Yield 0.063 g (87.50 %) IR (KBr, cm^{-1}): 3436 (OH), 3125 (NH), 2915 (C-H), 1712 (C=O), 1699 (COOPt), 1560 (NH) 1437, 1347 (Al-N), 996 (C-O), 737 (Na-O), 128 (Pt-O), UV-Vis (pH 8.2): λ_{max} log ϵ : 359 (4.22), 699 (5.23) nm. Calculated for $\text{Na}_2\text{C}_{40}\text{H}_{27}\text{N}_{14}\text{O}_{17}\text{AlPt}_3$ C, 29.71 N, 12.0; H 2.41 Found C, 30.32 N, 11.57; H, 3.56. MALDI-TOF MS: Calculated 1625.26; Found 1485.4 amu $[\text{M}-(2(\text{NaCOO})+\text{OH})]^-$. ^1H NMR (D_2O): $\delta = 9.7$ (18H, m, NH_3), $\delta = 2.74$ (1H, s, OH) aromatic protons were not obtained.

2.4.2 Aluminium bis (diammine platinum) octacarboxy phthalocyanine (OHAlOCPc-2Pt(NH_3)₂, Scheme 3.1)

The synthesis was done using a similar procedure to that employed for OHAlOCPc-3Pt(NH_3)₂ by keeping the molar ratio of the platinum to phthalocyanine at 3: 1.

Yield 0.072 g (150.01 %) IR (KBr, cm^{-1}): 3436 (OH), 3125 (NH), 2915 (C-H), 1712 (C=O), 1699 (COOPt), 1560 (NH) 1437, 1347 (Al-N), 996 (C-O), 737 (Na-O), 128 (Pt-O) UV-Vis (pH 8.2): λ_{max} log ϵ : 359 (4.15), 699 (5.18). Calculated for $\text{Na}_4\text{C}_{40}\text{H}_{21}\text{N}_{12}\text{O}_{17}\text{AlPt}_2$ C, 33.59 N, 11.75 ; H 1.50 Found C, 33.26 N, 11.33; H, 1.36. MALDI-TOF MS: Calculated 1448.06; Found 1361 amu $[\text{M}-(\text{Na}+\text{COO})]^-$. ^1H NMR (D_2O): $\delta = 9.7$ (18H, m, NH_3), $\delta = 2.74$ (1H, s, OH) aromatic protons were not obtained.

2.4.3 Aluminium *trikis* (diaqua platinum) octacarboxy phthalocyanine (OHAlOCPc-3Pt(H₂O)₂, Scheme 3.2)

Aqueous solutions of the sodium salt of OHAlOCPc (0.051 g, 0.055 mmol) and potassium tetrachloro platinate (0.076, 0.19 mmol) were mixed together and then stirred for 4 h at 50 °C, following literature methods [13, 37, 58, 59]. The solution was allowed to form a precipitate over 2 days. The precipitate was then filtered and washed with water, ethanol, acetone and ether.

Yield 0.067 g (93%), IR (KBr, nujol, cm⁻¹): 3436 (OH), 2915 (C-H), 1712 (C=O), 1699 (COOPt), 1437, 1347 (Al-N), 996 (C-O), 737 (Na-O), ¹H NMR (DMSO-*d*₆): δ = 8.24 (8H, s, Ar-H), δ = 2.54 (12H, d, H₂O-H), UV-Vis (DMSO): λ_{max} log ε: 362 (4.86), 705 (5.25) nm, UV-Vis (PBS): λ_{max} log ε: 322 (4.51), 695 (5.53) nm. MALDI-TOF MS: Calculated 1639.26; Found 1556.4 amu [M-((Na+COO)+OH)]⁻. Calculated for Na₂C₄₀H₂₁N₈O₂₃AlPt₃ C, 29.29 N, 6.83; H 1.29. Found C, 29.60 %; N, 7.52 %; H, 2.08 %.

2.4.4 Aluminium *tetrakis* (diaquaplatinum) octacarboxy phthalocyanine (OHAlOCPc-4Pt(H₂O)₂, Scheme 3.2)

According to literature [13, 37], a mixture of mono-, di- and trisubstituted complexes occurs, when a ratio of 1: 7 (Pc to $K_2[PtCl_4]$) is employed, hence the platination is done in two steps [37].

Step 1

Aqueous solutions of the sodium salt of OHAIOCPc (0.052 g, 0.049 mmol) was dissolved in deionised water (12 mL) and then methanol (100 mL) was added. A solution of $K_2[PtCl_4]$ (0.085, 0.20 mmol) was prepared in 50 % ethanol (200 mL). The solutions were quickly mixed and were stirred at room temperature for 3 h. The solution was then left to stand for 48 h, and the precipitate filtered off. The precipitate (which is the intermediate) was washed with water and allowed to dry. (Yield: 0.071 g).

Step 2

The dry precipitate from step 1 (0.071 g,) was dissolved in deionised water (20 mL) and methanol (80 mL). A solution of $K_2[PtCl_4]$ (0.083 g, 0.20 mmol) was prepared in 50 % ethanol (200 mL). The solutions were mixed and stirred for 3 h, and left to stand for 48 hrs. The solution was filtered and the precipitate was washed with

water, ethanol, acetone and ether. The product was dried under vacuum to yield an intense greenish black solid.

Yield 0.0783 g (88 %). IR (KBr, cm^{-1}): 3524 (OH), 2922 (C-H), 1715 (C=O), 1689 (COOPt), 1437, 1347 (Al-N), 996 (C-O), 737 (Na-O), ^1H NMR ($\text{DMSO}-d_6$): δ = 8.16 (8H,s, Ar-H), δ = 2.48 (16H, d, H_2O -H), UV-Vis (DMSO): λ_{max} log ϵ : 362 (3.44), 706 (4.88) nm. MALDI-TOF MS: Calculated 1844.26; Found 1786.24amu [M-((NaCOO)+OH)] $^-$. Calcd. For $\text{C}_{40}\text{H}_{25}\text{N}_8\text{O}_{25}\text{AlPt}_4$ C, 26.35 %; N, 6.14 %; H 1.27 %. Found C, 26.28; % N, 5.99; % H, 1.98 %.

2.4.5: Synthesis of Platinum nanoparticles

The platinum nanoparticles were synthesized following a modified method from reference [68].

$\text{Pt}(\text{acac})_2$ (0.21g , 0.54 mmol, acac =acetylacetonate), 1,2-hexadecanediol (0.54 g, 2.08 mmol) and diphenyl ether (25 mL) were added into a three necked flask. Under a nitrogen atmosphere, the mixture was heated under reflux for 10 min. Oleic acid (167 μL) and oleylamine (170 μL) were added as stabilizers and the mixture was refluxed for 20 min. The reaction was then cooled to room temperature. Ethanol (60 mL) was added to the solution and the black precipitate collected by centrifugation.

The product was washed with ethanol and then further dispersed in hexane (60 mL) solution containing stabilizers oleic acid (167 μ L) and oleylamine (170 μ L). The hexane was removed by centrifugation and the product was dried for 72 hrs in a vacuum. After drying the precipitate was washed with water (2 \times 50 mL) and ethanol (2 \times 50 mL). The precipitate was dried for 1 week.

Part of the results presented in this thesis has been published in a peer-reviewed journal and are listed below. The article is not referenced in this thesis

Synthesis and physicochemical behaviour of aluminium triakis and tetrakis (diaquaplatinum) octacarboxyphthalocyanine, NduduzoMalinga, Olga Dolotova, Roman Bulgakov, Edith Antunes, Tebello Nyokong, Dyes and Pigments., 95 (2012) 572.

CHAPTER THREE

RESULTS AND DISCUSSION

3.1 SYNTHESIS AND CHARACTERIZATION

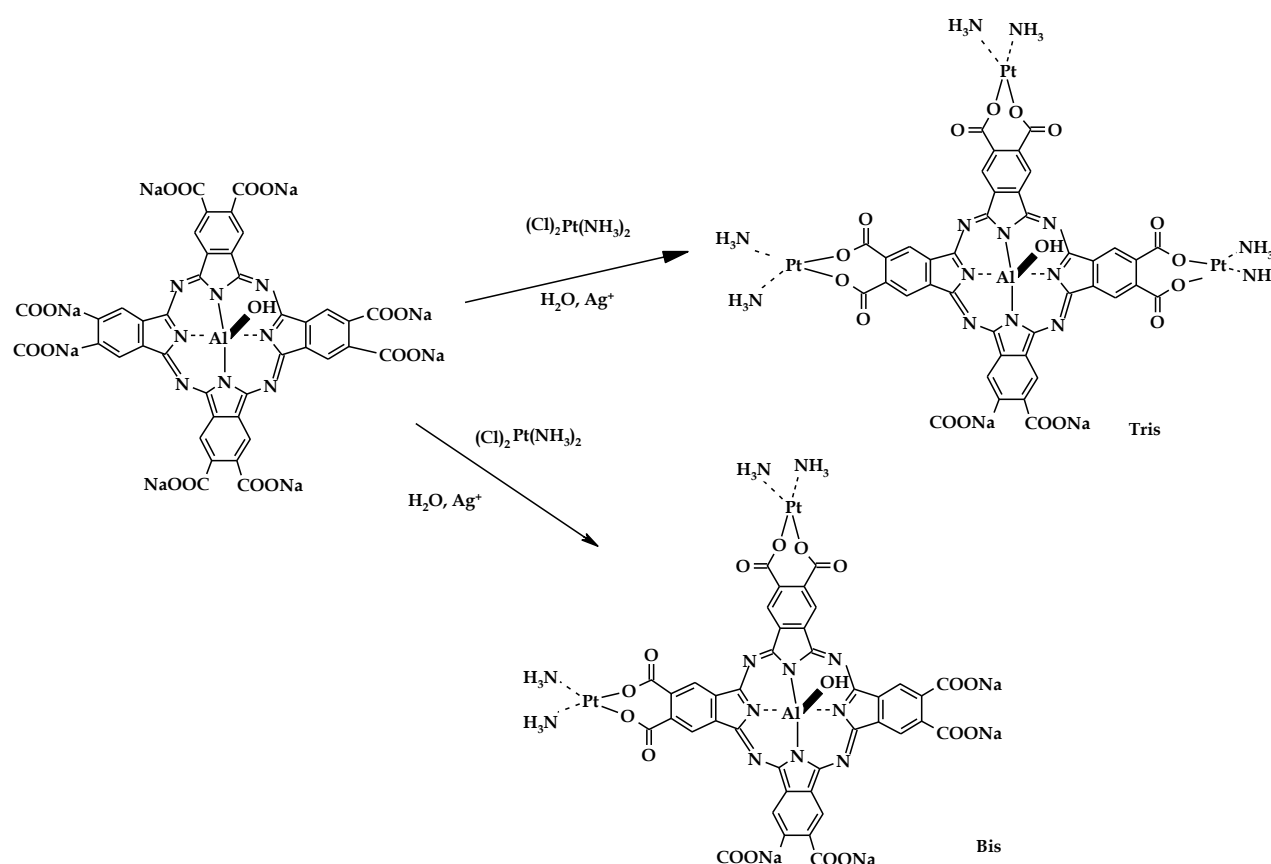
3.1.1 SYNTHESIS

3.1.1.1 Aluminium bis and tris (diammineplatinum) octacarboxy phthalocyanine, (Scheme 3.1)

The *cis*-diamminedichloroplatinum is only partially soluble in water. Hence an equimolar amount of AgNO₃ was added to solubilise the *cis*-diamminedichloroplatinum. The silver nitrate removed the chloro ligands and allowed the complex to be soluble. The conjugation of *cis*-diamminedichloroplatinum to OHAlOCPc to form OHAlOCPc-3Pt(NH₃)₂ or OHAlOCPc-2Pt(NH₃)₂ was carried out in water, without the addition of any organic solvents. The synthesis was carried out according to modified literature methods [38]. Both conjugates are soluble in basic media and not soluble in most organic solvents such as dimethyl sulfoxide. The solubility was found to be pH dependent. The complexes were not soluble below pH 8, thus a pH higher than this value (pH 8.2) was employed for all studies.

The complexes were characterized by various methods including ¹H NMR, IR, and UV-vis spectra as well as elemental analyses. The FTIR gave characteristic bands for the conjugates such as: O-H, N-H at (~3446 – 3500 cm⁻¹), (C=O (~1940 – 1750 cm⁻¹), PtCOO (1650 to 1699) C-O (~1170 – 1210 cm⁻¹), Na-O (705 cm⁻¹) which are concurrent with literature values [38,61]. The ¹H NMR obtained was not conclusive for these

compounds; this was due to partial solubility in deuterium oxide. The data obtained confirmed the presence of the ammine which appeared as multiplet at 9.7 ppm. However signals were not obtained for the aromatic region corresponding to phthalocyanine protons. A mass fragment of 1361 amu was obtained for $(\text{OH})\text{AlOCPc-2Pt}(\text{NH}_3)_2$ which corresponded to the loss of a sodium carboxylate group $[\text{M}-(\text{NaCOO})]$. No molecular ion peaks were observed for both complexes.



Scheme 3.1: Synthesis of aluminium bis and tris (diammineplatinum) octacarboxyphthalocyanine

The SEM-EDS of the conjugates $(\text{OH})\text{AlOCPc-3Pt}(\text{NH}_3)_2$ and $(\text{OH})\text{AlOCPc-2Pt}(\text{NH}_3)_2$ had expected ratios of 1:3 and 1:2 (Al:Pt), respectively (Table 3.1). Both

complexes gave excellent elemental analysis results confirming that they are pure and that there were no starting materials remaining in the product. From the elemental analyses, it was determined that there was no mixture of conjugate complexes.

The data obtained from elemental analysis for $(\text{OH})\text{AlOCPc-3Pt}(\text{NH}_3)_2$ was C, 29.60 % N, 7.52%; H, 2.08 % which corresponded with the actual elemental percentage of $(\text{OH})\text{AlOCPc-3Pt}(\text{NH}_3)_2$. The SEM-EDS was in agreement with elemental analyses and gave the elemental composition of 1.80 % Al, 4.69 % Na, 18.04 % O, 8.95 % N, 29.93 % C and 36.48 % Pt. The carbon percentage difference between the actual and experimental data is less than 1 % showing that the conjugates were very pure.

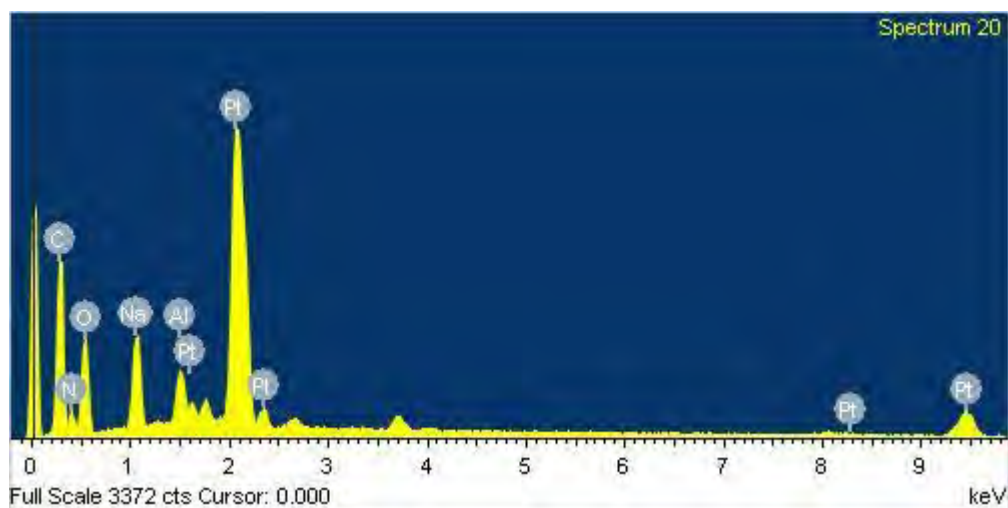
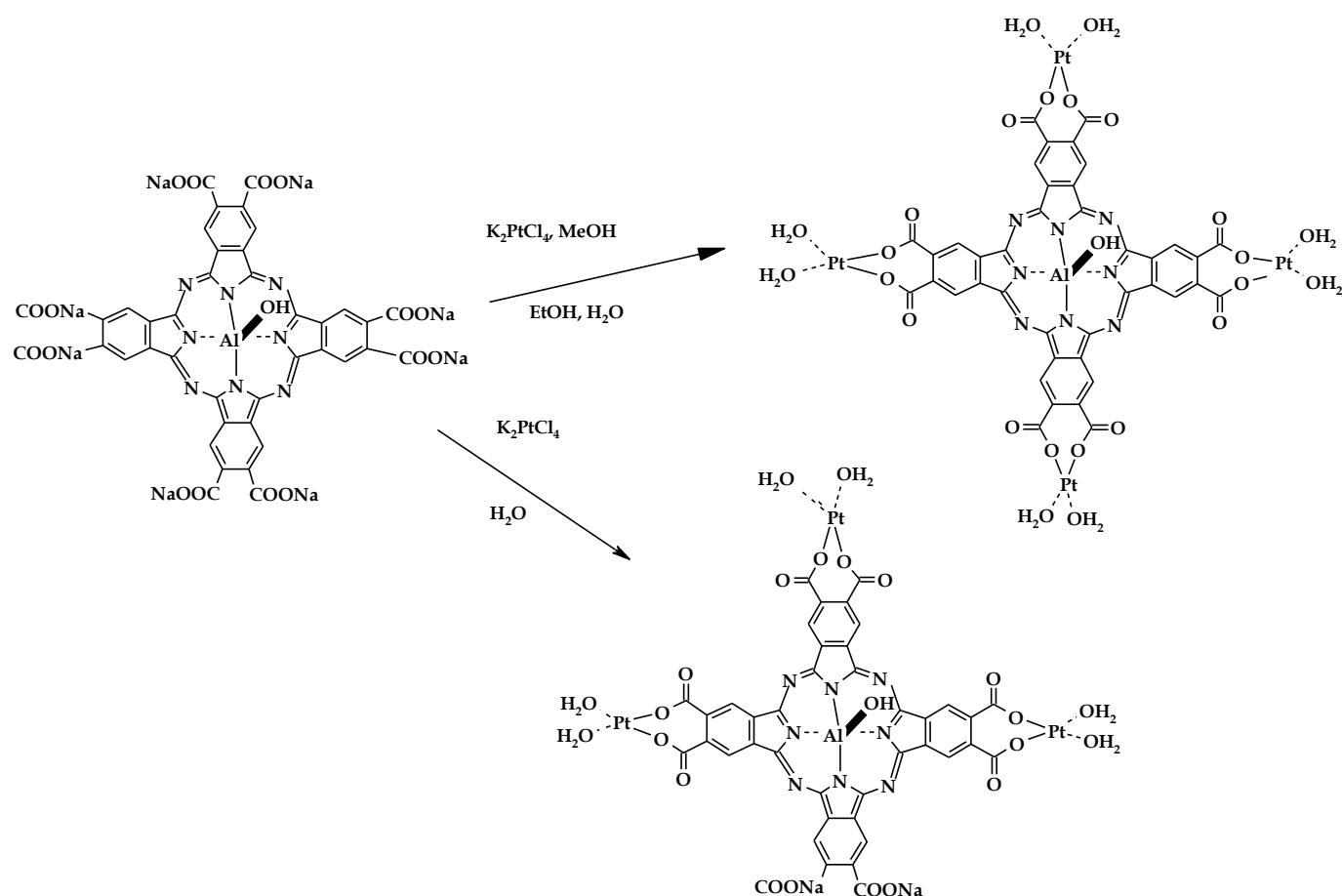


Figure 3.1: SEM-EDS data for $(\text{OH})\text{AlOCPc-3Pt}(\text{NH}_3)_2$ showing the different elements in the conjugate

3.1.1.2 Aluminium trikis and tetrakis (diaaquaplatinum) octacarboxyphthalocynine



Scheme 3.2: Synthesis of aluminium trikis and tetrakis (diaaquaplatinum) octacarboxyphthalocynine

$(OH)AlOCPc-3Pt(H_2O)_2$ was synthesized in a manner that was slightly different to that reported in the literature for $FeOCPc-4Pt(H_2O)_2$ derivatives [37, 58] (Scheme 3.2). The synthesis of $(OH)AlOCPc-3Pt(H_2O)_2$ was carried out in water only, without an organic solvent (methanol) as used in the literature [37]. Literature suggests that the formation of the Pt-O covalent bond retards solubility in water and thus influences changes in the physico-chemical properties of the complexes. The two remaining

COONa in (OH)AlOCPc-3Pt(H₂O)₂ allows the complex to be sparingly soluble in water. Elemental analyses confirmed the formation of the OHAlOCPc-3Pt(H₂O)₂ and OHAlOCPc-4Pt(H₂O) complexes, with the percentage carbon differing by less than 1 %.

The same trend was observed for (OH)AlOCPc-3Pt(H₂O)₂ and (OH)AlOCPc-4Pt(H₂O)₂. The data obtained from the SEM-EDS (Table 3.1) supported the data obtained from elemental analyses. It was found that the conjugates (OH)AlOCPc-3Pt(H₂O)₂ and (OH)AlOCPc-4Pt(H₂O)₂ had ratios of Al:Pt 1:3 and 1:4 respectively, which was expected.

Table 3.1: Table of Elemental composition of the conjugates obtained from SEM-EDS

Element	AlOCPc-3Pt(H ₂ O) ₂		AlOCPc-4Pt(H ₂ O) ₂		AlOCPc-3Pt(NH ₃) ₂		AlOCPc-2Pt(NH ₃) ₂	
	Atomic%	Weight%	Atomic%	Weight%	Atomic%	Weight%	Atomic%	Weight%
C	29.29	51.93	26.31	51.28	29.93	52.83	33.12	52.63
N	6.38	10.40	6.13	10.25	8.95	13.55	11.33	15.79
O	22.44	29.87	21.93	32.05	18.04	23.91	18.74	22.68
Na	2.81	2.60	-	-	4.69	4.32	6.34	5.26
Al	1.65	1.30	1.48	1.28	1.80	1.42	1.86	1.31
Pt	35.69	3.90	42.77	5.13	36.58	3.98	26.89	2.63
Al:Pt		1:3		1:4		1:3		1:2

3.1.2 Ultraviolet-Visible absorption, excitation and emission spectra

3.1.2.1 Aluminium octacarboxyphthalocyanine

The UV-Vis spectrum showed that the OHAlOCPc is monomeric in solution. This is evident by the single narrow Q-band (~694 nm in PBS) which is typical of metallated

octacarboxyphthalocyanine [36]. Figure 3.2 shows the absorbance spectra of the phthalocyanine and a red shift is observed when the solvent is changed from PBS to DMSO. It suspected that the DMSO stabilises the LUMO of the OHAIOCPc, thus the ground electronic spectra is red shifted [66].

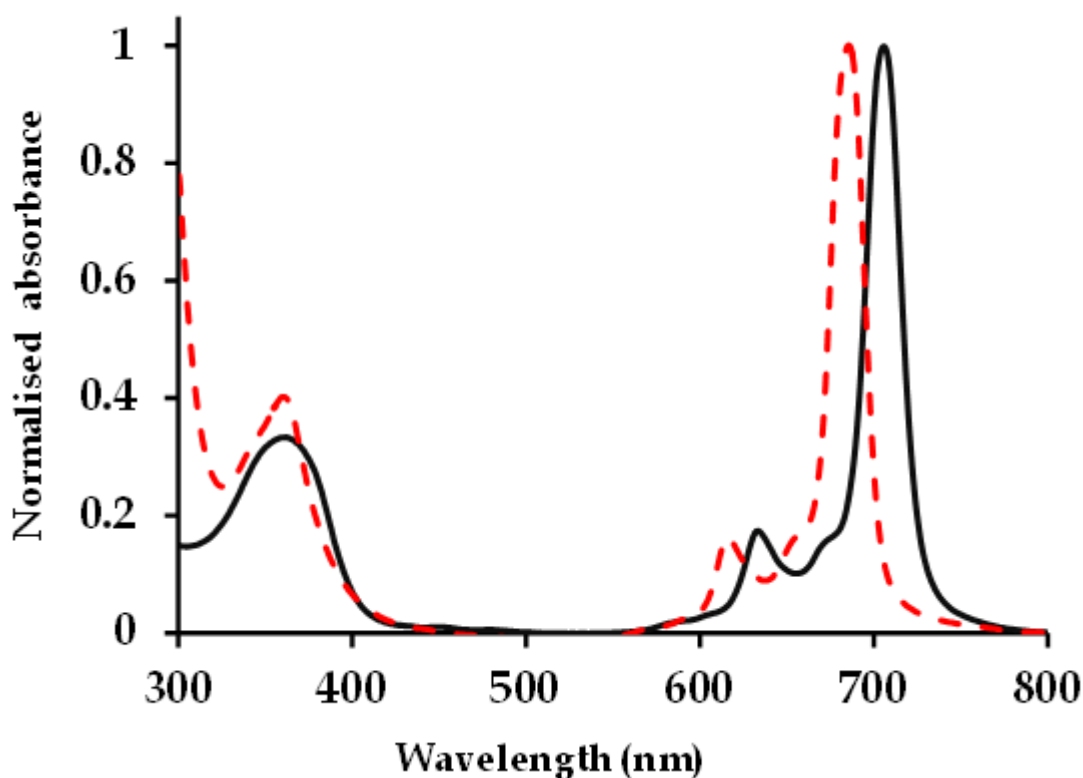


Figure 3.2: Ground state absorbance spectra of aluminium octacarboxy phthalocyanine in DMSO (solid black) and PBS (dotted red).

The red shifting is further observed in the fluorescence and excitation spectra (Table 3.2). The red shift in the Q-band is more prominent in DMSO which is the more basic compared to DMF and PBS.

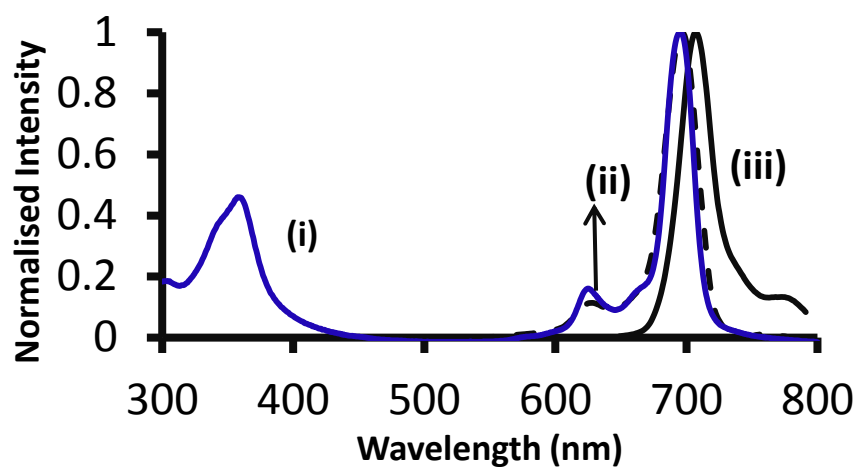


Figure 3.3: Absorption (i), excitation (ii) and emission (iii) spectra of (OH)AlOCPc in PBS .

Fig. 3.3 shows that there was no change in geometry upon excitation. This is evident by the similarity between absorbance and excitation spectra. There is a slight difference in the absorbance and excitation Q-band maximum due to the different instruments employed. There was no change in geometry upon excitation.

Table 3.2:Ground state absorprtion, flourescence emmission and extitation parameters for (OH)AlOCPc, (OH)AlOCPc-2Pt(NH₃)₂, (OH)AlOCPc-3Pt(NH₃)₂, (OH)AlOCPc-3Pt(H₂O)₂ and (OH)AlOCPc-4Pt(H₂O)₂ in different solvents

Complex	Solvent	Absorbance λ_{abs} (nm)	Excitation λ_{abs} (nm)	Emission λ_{emi} (nm)	Stokes shift Δ_{stokes}
OHAlOCPc	PBS	689	687	702	15
	DMF	699	698	709	11
	DMSO	704	702	711	9
	pH 8.2	696	694	706	12
(OH)AlOCPc-2Pt(NH ₃) ₂	pH 8.2	692	690	702	12
(OH)AlOCPc-3Pt(NH ₃) ₂	pH 8.2	690	688	701	13
(OH)AlOCPc-3Pt(H ₂ O) ₂	DMSO	706	705	711	6
	PBS	694	693	704	11
(OH)AlOCPc-4Pt(H ₂ O) ₄	DMSO	706	705	711	6

Fig. 3.4 shows the relationship between the concentration and absorbance. It shows monomeric behavior in concentrations between 9.22×10^{-6} to 1.2×10^{-5} mol. dm⁻³. Beer-Lambert's law is obeyed for (OH)AlOCPc in all solvents listed in Table 3.2.

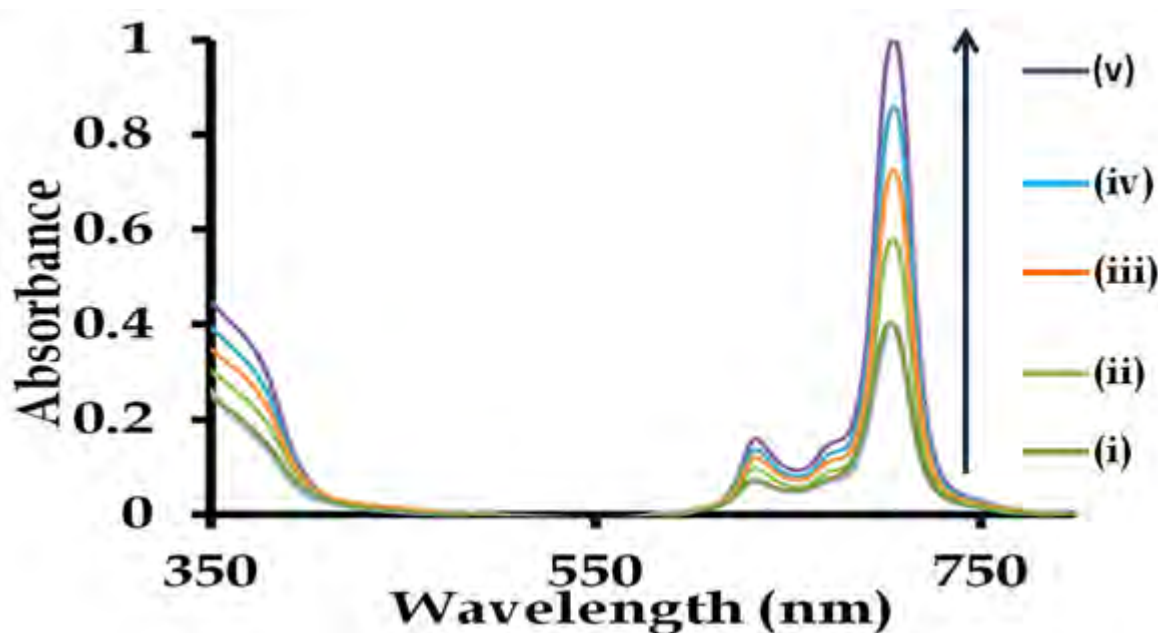


Figure 3.4: Ground state absorption spectra of (OH)AlOCPc at various concentrations: (i) = 9.22×10^{-6} , (ii) = 9.75×10^{-6} , (iii) = 1.06×10^{-5} , (iv) = 1.18×10^{-5} , and (v) = $1.28 \times 10^{-5} \text{ mol. dm}^{-3}$ in DMSO.

3.1.2.2. Aluminium tetrakis and triakis (diaquaplatinum) octacarboxyphthalocyanine

The spectrum of (OH)AlOCPc-4Pt(H₂O)₂ is similar to that of (OH)AlOCPc-3Pt(H₂O)₂ with the Q-band maxima at the same wavelength, (Table 3.2). There is a slight red shift in the Q-band of diaquaplatinum complexes compared to the plain OHAlOCPc in DMSO (Fig. 3.5 a). In PBS OHAlOCPc-3Pt(H₂O)₂ (Fig. 3.5 b) was slightly blue shifted.

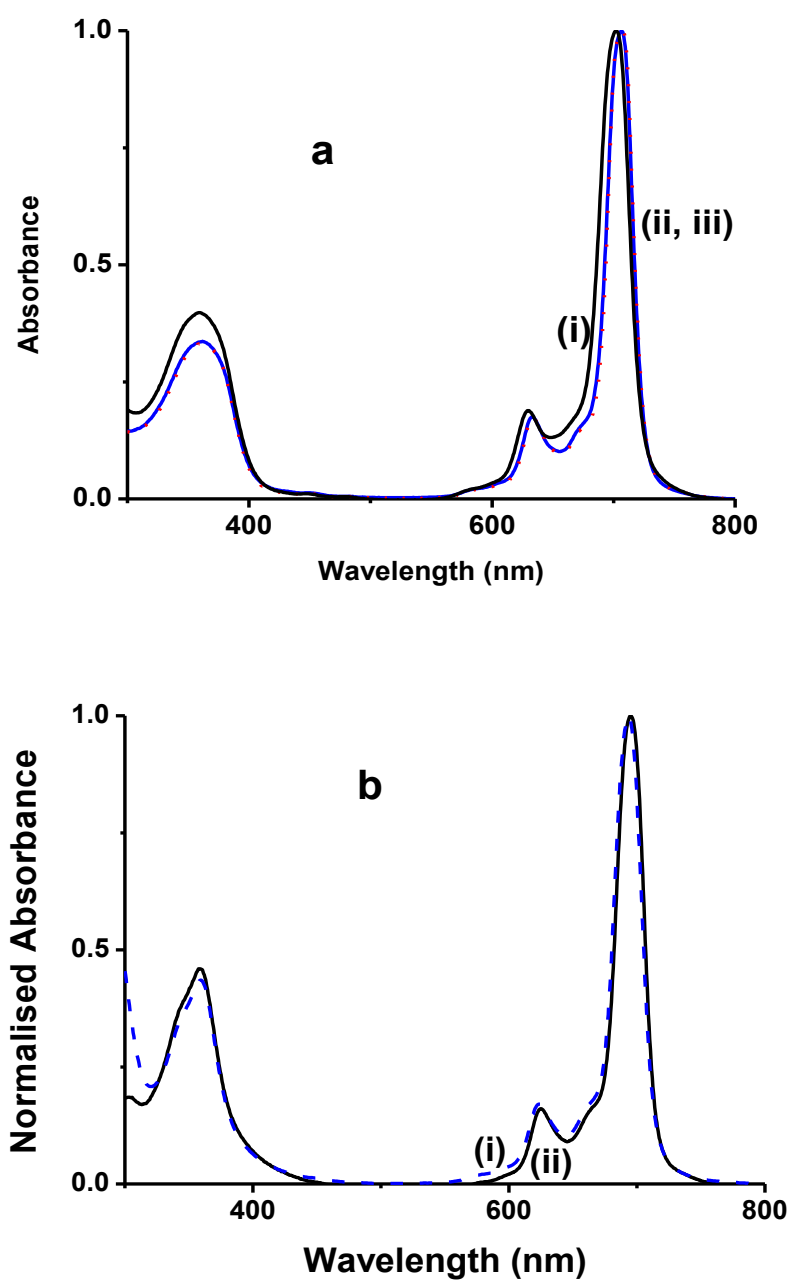


Figure 3.5: Comparative UV-visible spectra for (a) (OH)AlOCPc (i) (black solid) (OH)AlOCPc-3Pt(H₂O)₂ (blue solid) (ii) and (OH)AlOCPc-4Pt(H₂O)₂ (iii) (red dotted) in DMSO and (b) (OH)AlOCPc-3Pt(H₂O)₂ (blue dash) (i) and (OH)AlOCPc (black solid) (ii) in PBS. Concentration $\sim 1 \times 10^{-5}$ M.

In all the absorption spectra there was no significant change in the electronic spectra on platination as observed in literature for ZnOCPc-4Pt(H₂O)₂ and explained by modelling [60].

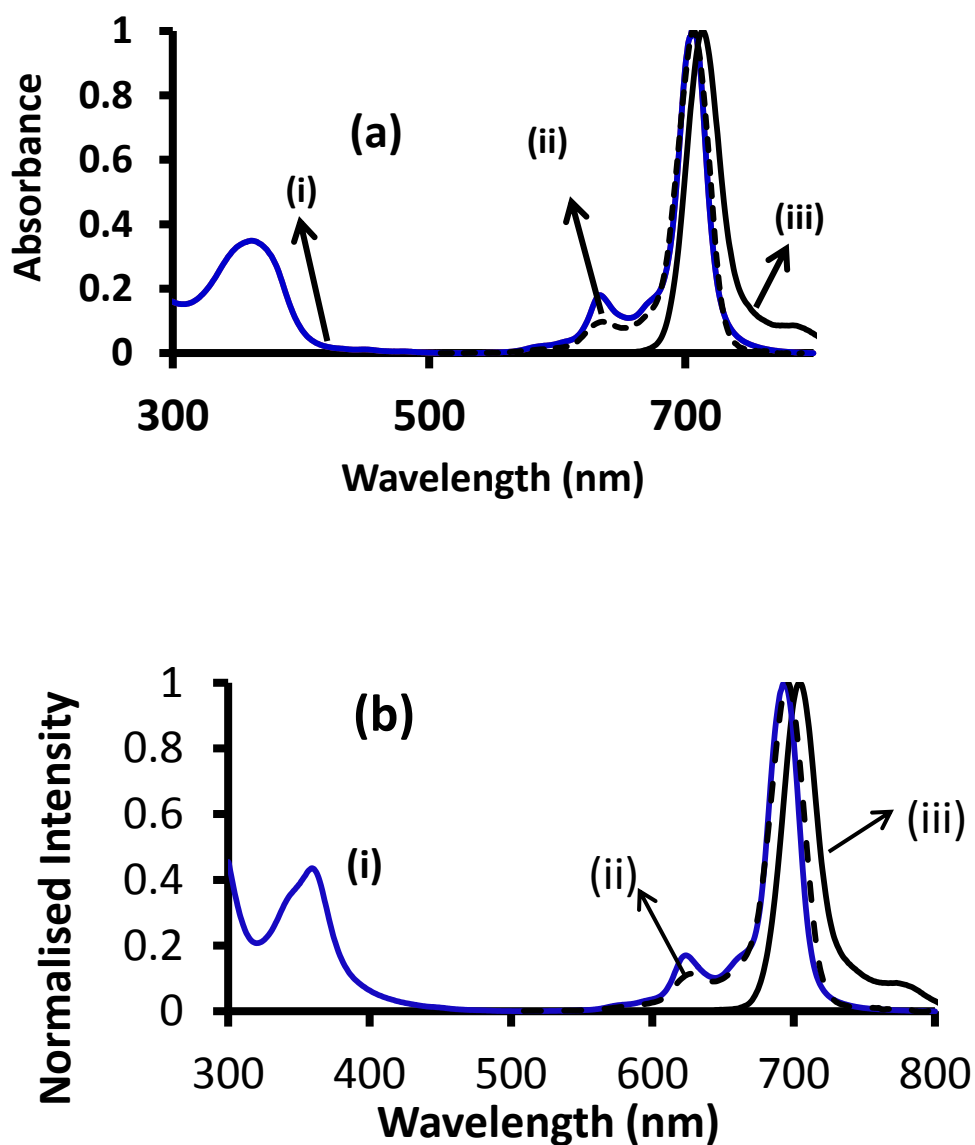


Figure 3.6: Absorption (i), excitation (ii) and emission (iii) spectra of (a) OHAIOCPc-4Pt(H₂O)₂ in DMSO and (b) OHAIOCPc-3Pt(H₂O)₂ in PBS.

The absorption spectra were similar to excitation spectra for both conjugates and the emission spectra were mirror images. Small differences were found in the absorption and excitation spectra which were due to differences in equipment employed.

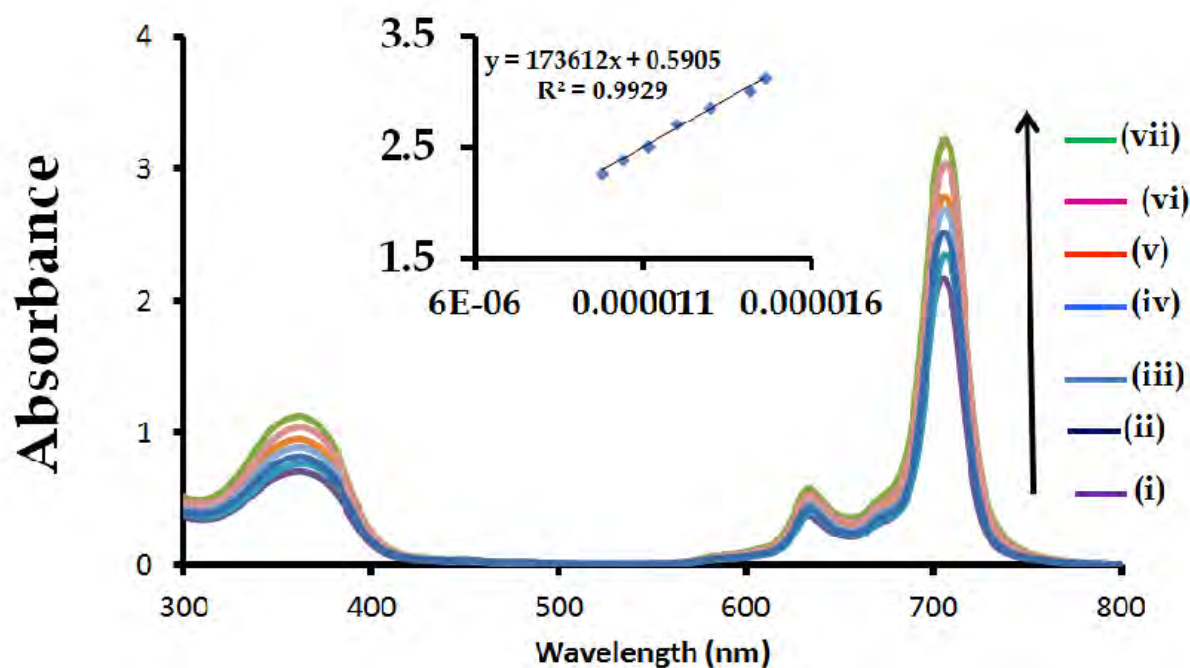


Figure 3.7: Ground state absorption spectra of (OH)AlOCPc-4Pt(H₂O)₂ at various concentrations: (i) = 9.78×10^{-6} , (ii) = 1.04×10^{-5} , (iii) = 1.11×10^{-5} , (iv) = 1.19×10^{-5} , (v) = 1.29×10^{-5} , (vi) = 1.41×10^{-5} and (v) = 1.46×10^{-5} mol. dm⁻³ in DMSO.

Fig. 3.7 shows the relationship between the concentration and absorbance. This also shows that there are no new bands forming, normally blue shifted due to the aggregated species. Beer-Lambert's law was obeyed for all the conjugates in the concentrations ranging from 9.78×10^{-6} to 1.46×10^{-5} mol. dm⁻³. This also suggests that the conjugates are monomeric in solution.

3.1.2.3. Aluminium tris and bis (diammineplatinum) octacarboxyphthalocyanine

Aluminium bis and tris (diammine platinum) octacarboxy phthalocyanines were found to be insoluble in common organic solvents such as: ethanol, DMSO, DMF and dichloromethane. Thus UV-Vis and fluorescence data was obtained in pH 8.2 (Fig. 3.8). The data shows that there was a slight blue shift upon conjugation (Table 3.2). But essentially there is no significant change in the electronic spectra on platination. It has been shown in literature [60] that there are no changes in the Q-band.

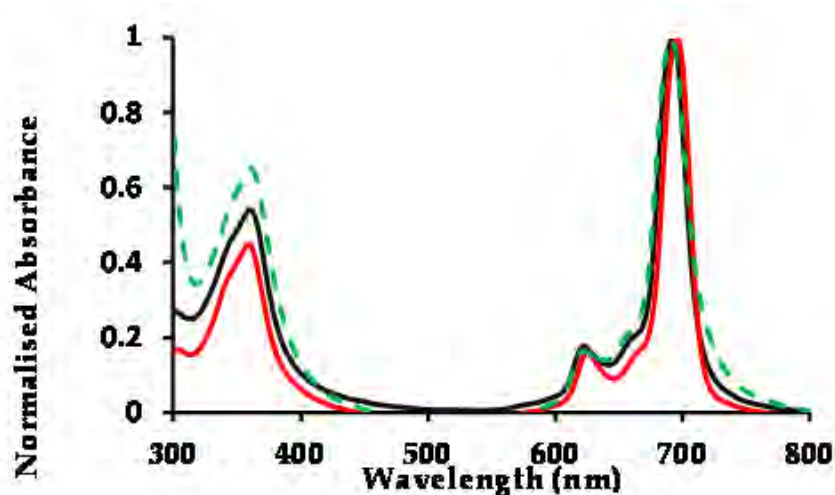


Figure 3.8: Ground state absorbance spectra of (OH)AlOCPc (solid red), (OH)AlOCPc-2Pt(NH₃)₂(solid black) and (OH)AlOCPc-3Pt(NH₃)₂(dotted green) in pH 8.2.

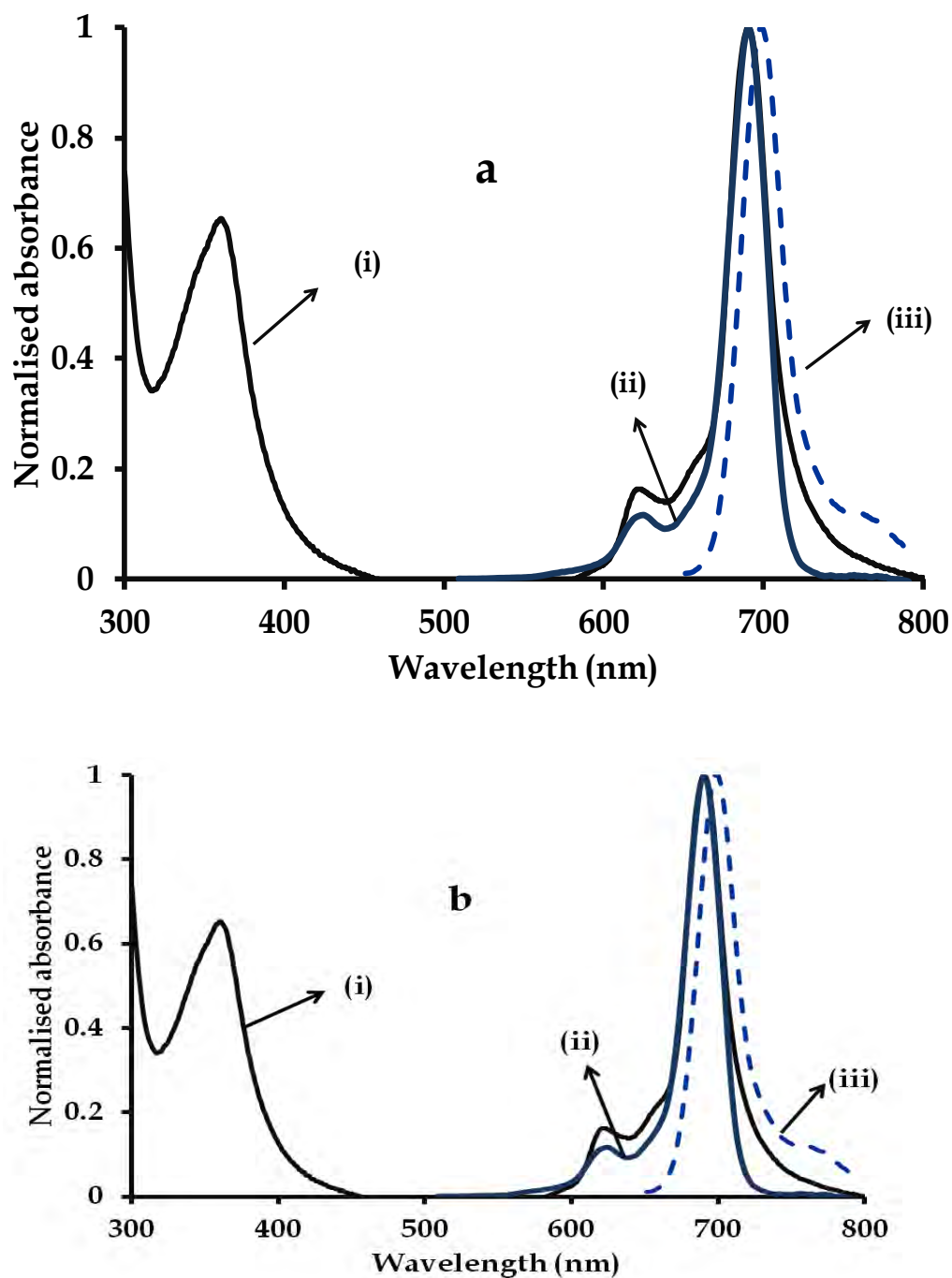


Figure 3.9: Absorption (i), excitation (ii) and emission (iii) spectra of (a) OHAIOCPc-3Pt(NH₃)₂ in pH 8.2 and (b) OHAIOCPc-2Pt(NH₃)₂ in pH 8.2.

The absorption was similar to excitation spectra for both conjugates and the emission spectra were mirror images (Fig. 3.9). Small differences were found between absorption and excitation spectra due to differences in equipment employed.

3.1.3 Powder X-ray Diffraction and Transmission Electron Microscopy

It has been reported that the conjugation of octacarboxy phthalocyanine with K_2PtCl_4 forms platinum nanoparticles [58, 59]. Thus platinum nanoparticles were synthesized for comparison with $OHAlOCPc-3Pt(H_2O)_2$ and $OHAlOCPc-4Pt(H_2O)_2$. The XRD spectra were employed to confirm the formation of platinum nanoparticles for $OHAlOCPc-3Pt(H_2O)_2$ or $OHAlOCPc-4Pt(H_2O)_2$, (Fig 3.10). The $OHAlOCPc$ had one peak at $2\theta = 26^\circ$ which is characteristic of Pcs [69-71]. From the XRD spectrum, $OHAlOCPc$ has both amorphous and crystalline properties as judged by the sharp and broad base peaks. It has been reported before in literature the MPc are amorphous [71].

Comparison with the International Centre for Diffraction Data (ICDD) database, showed that the $OHAlOCPc-3Pt(H_2O)_2$ and $OHAlOCPc-4Pt(H_2O)_2$ complexes have patterns that fit the platinum nanoparticles peak positions. This was also shown by the XRD of the Pt nanoparticles in Fig. 3.10 that were synthesised for comparison. The peaks around $2\theta = 40^\circ, 46^\circ, 69^\circ, 82^\circ$ and 87° belong to platinum with 99.9 % fit. A similar XRD pattern was observed for the corresponding $FeOCPc-4Pt(H_2O)_2$ and a

very broad Pc XRD peak [58] was obtained. Pt nanoparticles peaks were observed at $2\theta = 40^\circ, 47^\circ, 69^\circ$ and 86° , and corresponded to the literature values. However the peak at 67° was not observed in literature [58].

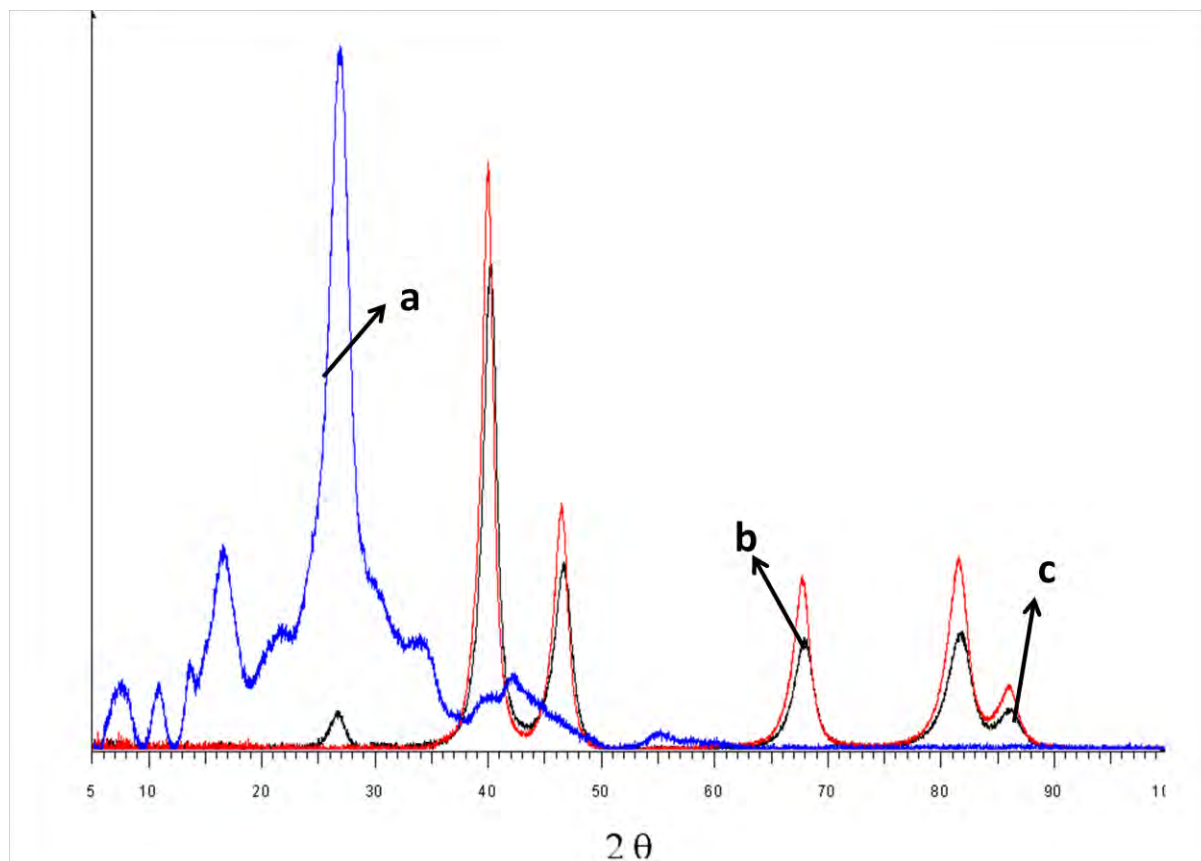


Figure 3.10: Comparative XRD spectrum for OHAIOCPc (a), Pt nanoparticles (b) and OHAIOCPc-3Pt(H₂O)₂(c).

The sizes of the Pt conjugate (deemed to be nanoparticles by the appearance of broad peaks corresponding to platinum) were determined using XRD data and the Debye-Scherrer [72] Equation 3.1:

$$d(\text{\AA}) = \frac{k\lambda}{\beta \cos \theta} \quad (3.1)$$

where k is an empirical constant equal to 0.9, λ is the wavelength of the X-ray source, (1.5405 Å), β is the full width at half maximum of the diffraction peak, and θ is the angular position of the peak. The size of particles of OHAlOCPc-3Pt(H₂O)₂ was found to be 7.9 nm and 5.8 nm for OHAlOCPc-4Pt(H₂O)₂, confirming aggregation of platinated phthalocyanine complexes as observed before [58] or the formation of Pt nanoparticles with the Pc acting as stabilisers. The size of Pt nanoparticles used for comparison in this work was found to be 3.4 nm. The transmission electron microscopy shows the formation of platinum nanoparticles for the conjugate. The photomicrograph (Fig 3.11) showed that the platinum nanoparticles formed were aggregated.

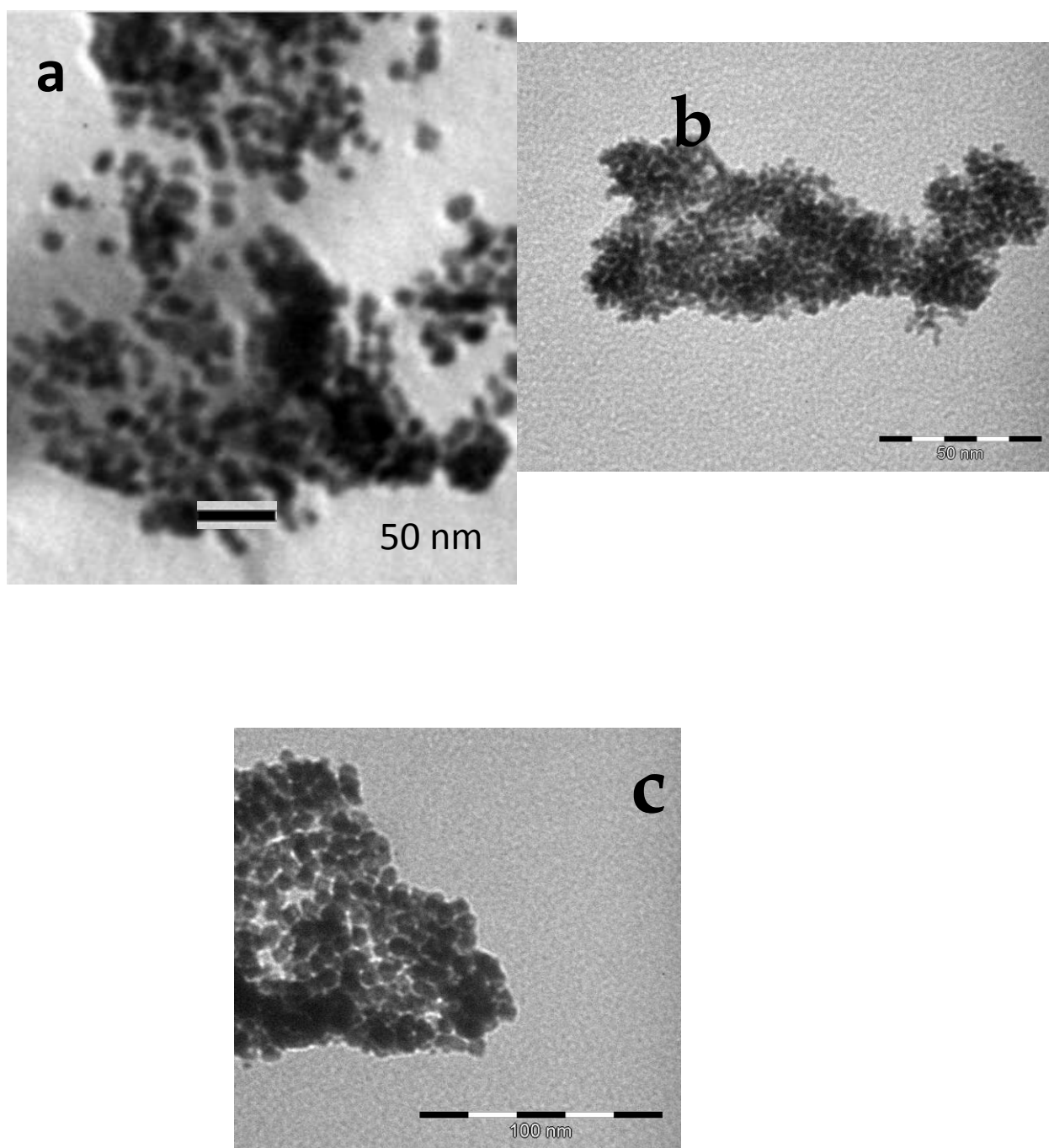


Figure 3.11: TEM images of platinum nanoparticles (a), $\text{OHAIOCPc-3Pt(H}_2\text{O)}_2$ (b) and $\text{OHAIOCPc-4Pt(H}_2\text{O)}_2$ (c).

The conjugates that were prepared from cis-diamminedichloroplatinum did not form nanoparticles as confirmed by the XRD, (Fig. 3.12) and showed relatively broad peaks suggesting an amorphous nature [70] upon conjugation in both OHAlOCPc-3Pt(NH₃)₂ and Al(OH)OCPc-2Pt(NH₃)₂ (the latter shown in Fig. 3.12).

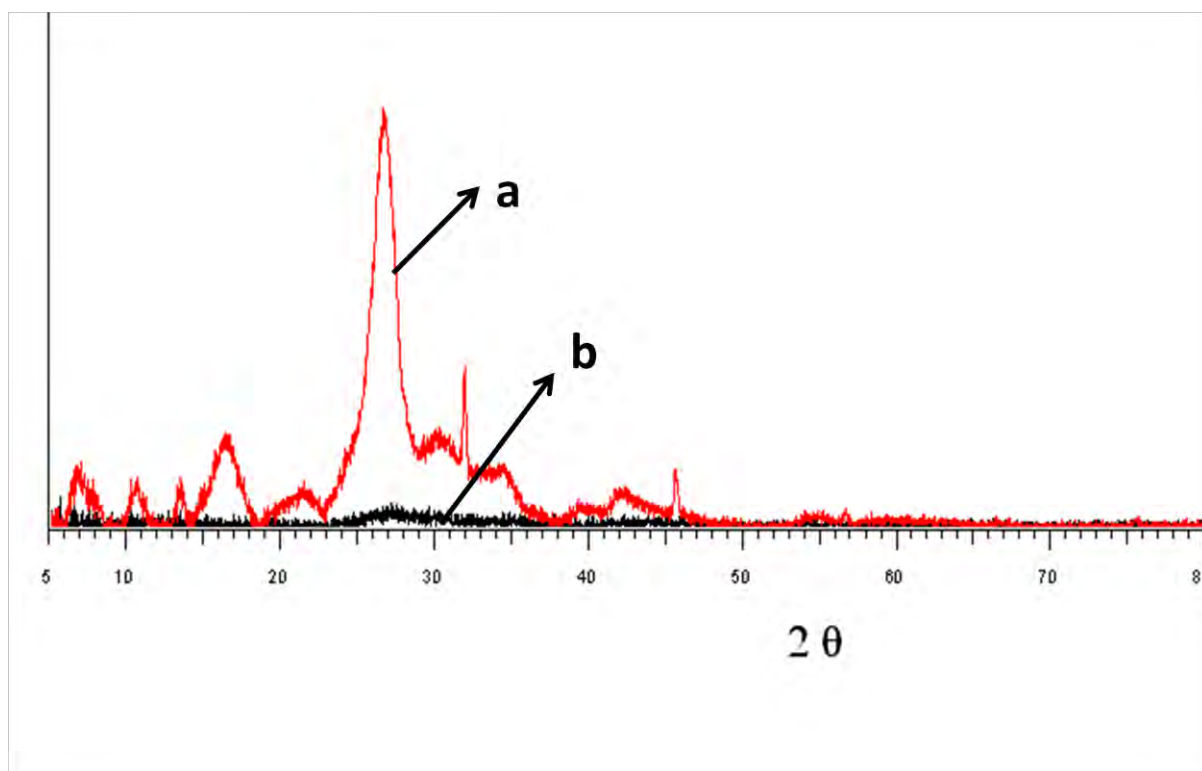


Figure 3.12: Comparative XRD spectra for (OH)AlOCPc (a) and (OH)AlOCPc-3Pt(NH₃)₃ (b).

3.2 PHOTOPHYSICAL PARAMETERS

3.2.1. Fluorescence lifetime (τ_F) and quantum yields (Φ_F)

The fluorescence quantum yield (Φ_F) for all four complexes are listed in Table 3.3. The $\text{OHAIOCPc-3Pt(NH}_3)_2$, $\text{OHAIOCPc-2Pt(NH}_3)_2$, $\text{OHAIOCPc-3Pt(H}_2\text{O)}_2$ and $\text{OHAIOCPc-4Pt(H}_2\text{O)}_2$ had Φ_F values that were lower than that of OHAIOCPc . This was expected due to the fact that the presence of the platinum in the conjugates encourages intersystem crossing, lowering the fluorescence quantum yield due to the heavy atom effect. The Φ_F is largely affected by factors such as: temperature, structure, solvent parameters (polarity, viscosity and refractive index) and the presence of heavy atoms in the sample. The heavy platinum ions have a high spin orbit coupling which causes a spin flip into the triplet state, resulting in lowering of the fluorescence quantum yield. The Φ_F values in water are much lower than in DMSO probably due to the higher viscosity of DMSO compared to water [66, 73, 74]. A viscous solvent like DMSO reduces the translational and rotational motions in the MPc complexes. It has been established in literature that the fluorescence of a sample is a function of the viscosity of solvent that the sample is dissolved in [74]. The Φ_F in PBS was 0.06 and 0.15 in DMSO for $\text{OHAIOCPc-3Pt(H}_2\text{O)}_2$; which was soluble in both solvents. The photophysical properties values for OHAIOCPc in PBS used were cited from literature [75].

Table 3.3: Table of triplet state parameters for (OH)AlOCPc and its platinated derivatives

Sample	Solvent	Φ_F	Φ_T	Φ_{IC}	$\tau_F(\text{ns})^a$ ± 0.01	$\tau_T(\mu\text{s})$	Ref
(OH)AlOCPc	DMSO	0.23	0.20	0.57	5.26(100%)	756	TW
	PBS	0.27	0.32	0.41	4.45(100%)	450	75
	pH 8.2	0.12	0.28	0.60	4.37(100 %)	25	TW
(OH)AlOCPc-3Pt(H ₂ O) ₂	DMSO	0.15	0.45	0.40	5.46 (100%)	577	TW
	PBS	0.06	0.36	0.58	4.09 (100%)	36	TW
(OH)AlOCPc-4Pt(H ₂ O) ₂	DMSO	0.05	0.57	0.42	5.34 (92.4%)	526	TW
					1.51(7.6%)		
(OH)AlOCPc-2Pt(NH ₃) ₂	pH 8.2	0.08	0.34	0.58	4.23 (93%)	18	TW
					1.32 (7%)		
(OH)AlOCPc-3Pt(NH ₃) ₂	pH 8.2	0.02	0.42	0.56	4.28 (91%)	14	TW
					1.45 (9%)		

^aAbundances in brackets. ^bTW= this work.

The fluorescence lifetimes were recorded using TCSPC, (Fig. 3.13). A mono-exponential decay (Table 3.3) was observed for (OH)AlOCPc, indicating that there is only one species in the solution. The lifetimes were within the range reported for phthalocyanines [76]. (OH)AlOCPc-3Pt(H₂O)₂ showed a mono-exponential decay with one lifetime in both DMSO and water. While a bi-exponential decay was obtained for (OH)AlOCPc-4Pt(H₂O)₂, (OH)AlOCPc-3Pt(NH₃)₂ and (OH)AlOCPc-2Pt(NH₃)₂. The longer (unquenched) lifetime is attributed to the monomer and the shorter lifetime is attributed to the quenched lifetime, (quenched by the dimmer) [77]. The second component was of low abundance.

Time resolved emission spectra (TRES) was carried out in DMSO (Fig 3.14). This method confirmed two emitting species for OHAlOCPc-4Pt(H₂O)₂ with emission wavelengths at 711 and 709 nm, the former is similar to that observed for OHAlOCPc-4Pt(H₂O)₂ (Table 3.2). For (OH)AlOCPc-2Pt(NH₃)₂ it is suspected that the second emitting species could be one of the two isomers that exist. (OH)AlOCPc-2Pt(NH₃)₂ can exist as cis and trans isomers giving rise to two emitting species and thus a bi-exponential decay is observed.

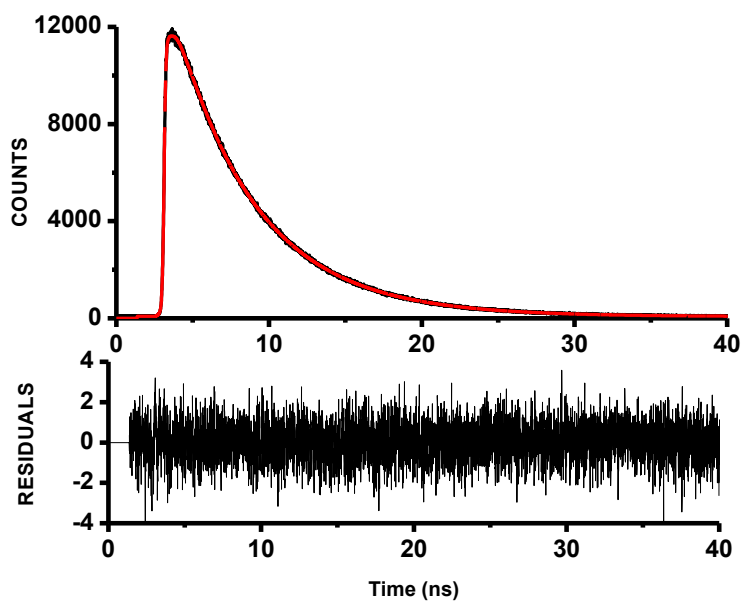


Figure 3.13: Typical TCSPC decay curve for (OH)AlOCPc-4Pt(H₂O)₂ in DMSO.

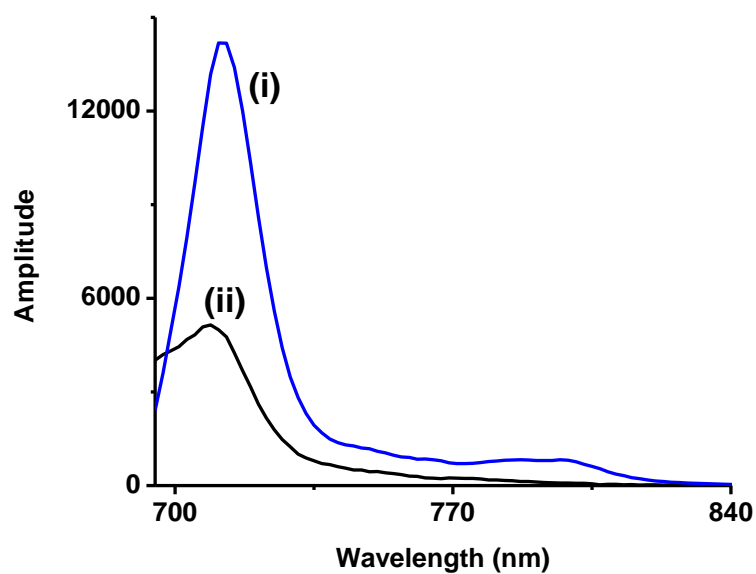


Figure 3.14: Typical TRES spectrum for OHAlOCPc-4Pt(H₂O)₂ showing deconvoluted emission peaks in DMSO. (i) unquenched and (ii) quenched fluorescence.

3.2.2. Triplet state parameters.

The number of the absorbing molecules that undergo intersystem crossing (ISC) to the triplet state is a measure of the triplet state quantum yield. The efficiency of a phthalocyanine as a photosensitizer is determined by its triplet state quantum yield (Φ_T) and lifetime (τ_T). The triplet quantum yields (Table 3.3), were determined using the laser flash photolysis set up shown in the experimental section (Chapter 2) and calculated using Equation 1.2 as discussed in Chapter 1.

A representative transient differential spectrum and triplet decay curve (insert) for (OH)AlOCPc-3Pt(H₂O)₂ in DMSO is shown in Fig. 3.15. The transient spectra (Fig 3.15) obtained showed the same features as the absorption spectra.

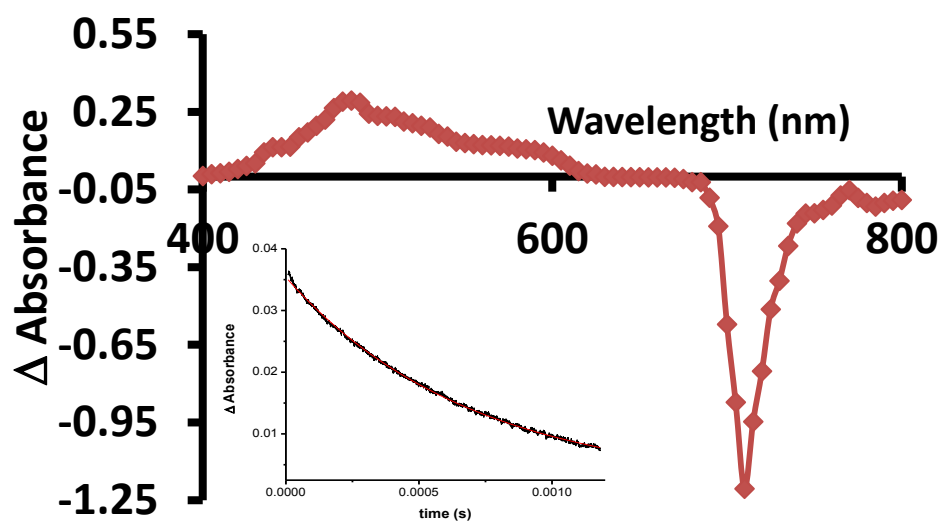


Fig. 3.15: A transient differential spectrum and inset: triplet decay curve of OHAIOCPc-3Pt(H₂O)₂DMSO. (Excitation wavelength = 692 nm in DMSO).

The triplet decay curve (Fig. 3.15 insert), followed a mono exponential fit. The triplet lifetimes are affected by oxygen, therefore in this thesis the solutions for triplet measurements were de-aerated sufficiently under argon before recording flash photolysis traces.

The triplet state parameters of conjugates such as (OH)AlOCPc-4Pt(H₂O)₄ and (OH)AlOCPc-3Pt(H₂O)₂ were determined in DMSO, (OH)AlOCPc-3Pt(H₂O)₂ was determined in PBS. pH 8.2 was employed for (OH)AlOCPc-3Pt(NH₃)₂ and (OH)AlOCPc-2Pt(NH₃)₂ conjugates. The solvent used plays a huge role in the value

of the triple state parameters. The highest triplet lifetimes and quantum yields for the samples occurred in DMSO. The viscosity of DMSO impedes molecular deactivation. The molecular deactivation arises from molecular movements and vibration which are prominent in aqueous solvents such as PBS and pH 8.2.

In DMSO the triplet lifetime for (OH)AlOCPc was the highest at 756 μ s. There was a significant decrease in the lifetime when the solvent was changed from DMSO to PBS or pH 8.2. The lifetimes were quenched as a result of molecular deactivation in aqueous solvents. This trend was also observed in (OH)AlOCPc-3Pt(H₂O)₂ in DMSO the triplet lifetime was 577 and 36 μ s in PBS (Table 3.3). For (OH)AlOCPc-3Pt(H₂O)₂ and (OH)AlOCPc-4Pt(H₂O)₂ in DMSO, there is a decrease in lifetimes with an increase in platination. (OH)AlOCPc-3Pt(NH₃)₂ and (OH)AlOCPc-2Pt(NH₃)₂ had quenched triplet lifetime because the studies were determined in aqueous media. The lifetimes were in the range of 14 to 18 μ s (Table 3.3). For all the conjugates there was decrease in the lifetimes upon conjugation. This is expected due to the heavy atom effect exerted by Pt. The triplet lifetimes decreased with an increase in the number of platinum groups in Table 3.3, corresponding to the increase in Φ_T . The triplet quantum yields increased upon conjugation, due to the presences of the heavy platinum ions. In aqueous media there was a decrease in the triplet quantum yields due to solvent effects. This is due to [44] quenching of the triplet state of phthalocyanines by aqueous media.

The quantum yields of internal conversion (Φ_{IC}) were calculated using Equation 3.2. which assumes that only three processes (fluorescence, intersystem crossing and internal conversion), jointly deactivate the excited state of a molecule.

$$\Phi_{IC} = 1 - (\Phi_F + \Phi_T) \quad (3.2)$$

Internal conversion is the radiationless transition between energy states of the same spin state. The values of Φ_{IC} indicate the extent to which the excited molecules can be deactivated by increasing the thermal energy of their surroundings. The values obtained (Table 3.3) for Φ_{IC} did not have a pattern.

3.3 Singlet oxygen

Singlet oxygen quantum yields are determined by monitoring the degradation of a singlet oxygen quenchers such as DPBF or ADMA. The decrease of DPBF was monitored at 417 nm in DMSO, (Fig 3.16) The rate at which the DPBF degrades is related to the production of singlet oxygen. Figure 3.16 shows the decay of DPBF. There is no change in the Q-band showing no degradation of the Pc.

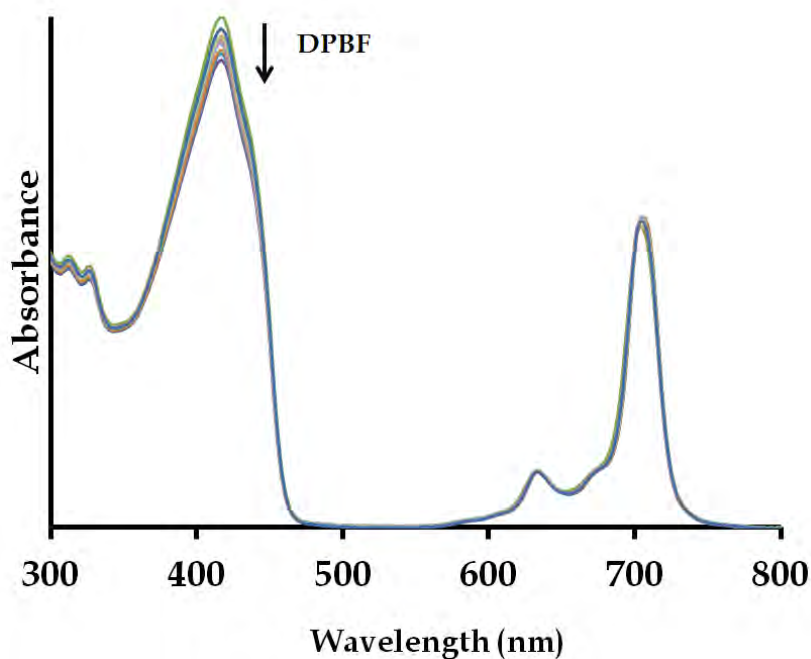


Figure 3.16: Photodegradation of DPBF in the presence of (OH)AlOCPc(PtH)₃ in DMSO.

The singlet oxygen quantum yields (Φ_{Δ}) were calculated using Equation 1.4 as mentioned in Chapter 1. An increase in triplet yield is expected to result in a corresponding increase in Φ_{Δ} for the platinated complexes compared to OHAlOCPc. This is observed in Table 3.4. In PBS and pH 8.2 the singlet oxygen quantum yields were lower than those were that obtained in DMSO, for reasons discussed above.

S_{Δ} is the measure of the efficiency of the excitation energy transfer from the triplet photosensitizer molecule to ground state (triplet) molecular oxygen, $^3\text{O}_2$. It is calculated from Equation 3.3.

$$S_{\Delta} = \Phi_{\Delta} / \Phi_T \quad (3.3)$$

The values reveal that the energy transfer to O₂ is more efficient upon platination,

Table 3.4.

Table 3.4: Singlet oxygen quantum yields of (OH)AlOCPc and its derivatives in a variety of solvents

Sample	Solvent	λ_{abs} nm	Φ_{Δ}	S_{Δ}
(OH)AlOCPc	DMSO	704	0.15	0.75
	PBS	696	0.12	0.38
	pH 8.2	689	0.12	0.34
(OH)AlOCPc-3Pt(H ₂ O) ₂	DMSO	706	0.38	0.84
	PBS	694	0.25	0.69
(OH)AlOCPc-4Pt(H ₂ O) ₂	DMSO	706	0.48	0.84
(OH)AlOCPc-2Pt(NH ₃) ₂	pH 8.2	699	0.23	0.67
(OH)AlOCPc-3Pt(NH ₃) ₂	pH 8.2	700	0.34	0.81

CHAPTER FOUR

CONCLUSIONS

4.1 GENERAL CONCLUSIONS

In this work, the aim is to achieve combination therapy for cancer treatment with the use phthalocyanine and platinum compounds. The OHAlOCPc was conjugated with K_2PtCl_4 and cis-diamminedichloroplatin to make cis-diammine-(1,1-cyclobutane dicarboxylato)platinum analogues for possible use in combination therapy. The phthalocyanines are the PDT agent while the platinum compounds are chemotherapy agents. The conjugates that were prepared gave satisfactory spectroscopic results which confirmed their purity. All of the prepared compounds exhibited monomeric behaviour in aqueous solution and in DMSO. In aqueous solvents the triplet lifetimes were quenched for all samples. In DMSO the values of the triplet lifetime for OHAlOCPc was 756 μs which was the high when compared to the lifetimes found in pH 8.2 (25 μs). OHAlOCPc-3Pt(H₂O)₂ whilst OHAlOCPc-4Pt(H₂O)₂ had a triplet lifetimes of 526 μs in DMSO and OHAlOCPc-3Pt(H₂O)₂ had triplet lifetime of 36 μs in PBS. OHAlOCPc-3Pt(NH₃)₂ and OHAlOCPc-2Pt(NH₃)₂ had triplet lifetimes of 14 and 18 μs , respectively. The results also showed that due to heavy atom effect, the triplet lifetimes decreased. In contrast, the triplet state quantum yields were higher in the platinated species. For all of the platinated species had triplet quantum yields were greater 0.3 which showed that the platination improved the efficiency of the phthalocyanine as a photosensitizer. The trend of the heavy atom effect improving the triplet state was observed in the fluorescence properties and singlet oxygen generation. The singlet oxygen quantum

yields improved upon platination. This shows that the conjugation with platinum improves the singlet oxygen quantum yields of the phthalocyanine. Based on the solubility of the compounds in aqueous solvents and their excellent photophysical behaviour, they have potential to be used in photodynamic therapy of cancer.

4.2 FUTURE PERSPECTIVE

Due to the good photophysical properties of the prepared conjugates, they may be investigated for dye sensitised solar cells. The octacarboxy phthalocyanines have been reported to have high photobleaching rates, thus the conjugate may be tested for photobleaching in order to investigate the effects of platination. Cell studies are needed to determine the potency of the platinum complex on cancerous cells and be compared with cis-diammine-(1,1-cyclobutanedicarboxylato)platinum for selectivity and potency studies.

REFERENCES

1. D.Bernad, D. Errante, U. Tirelli, L. Salvag, A. Bianco, I. S Fentiman, Cancer treatment reviews, 32 (2006) 277.
2. M. Mohiuddin, K. L. Zietzer, D. J. Moyland, R. M. Yelovich, L. Rose, Lung Cancer, (1995) 57.
3. J. D. Schoenfeld, J. R. Harris, The Breast, S3 (2011) S116.
4. D.C. Ash. J. Clin. Oncol., 10 (1980) 55
5. R. Bonnet, *Chemical aspects of photodynamic therapy*, Gordon and Breach Science Publishers, Germany , 2000.
6. J.D. Spikes, J.Photochem.Photobiol. B, 6 (1990) 259.
7. R.R. Allison, G. H Downie, R. Cuenca, X. Hu, C.J.H. Childs, C.H Sibata, PhotodiagnPhotodynTher., 1 (2004), 27.A. Bruan, J. Tcherniac, J. Ber. Dscht. Chem. Ges, 40 (1907) 2709.
8. J. He, H.E. Larkin , Y-S. Li, B.D. Rihter, S.I.A. Zadi, M.A.J. Rodgers, H. Mukhtar, M.E. Kenney, N.L. OLeinick, Photochem. Photobiol.B., 65 (1997) 581.
9. E.U. Lukyanets, J. Porphyrins. Phthalocyanines., 3 (1994) 4234
10. C.M. Allen, W.M. Sharman, J.E. van Lier, J. Porphyrins. Phthalocyanines., 5 (2001) 161.
11. C. Hadjur, G. Wagnières, F. Ihringer, P. Monnier, H. van den Bergh Ochsner, J. Photochem. Photobiol. B., 38 (1997) 196.

12. P. Garnuszek, I. Licianska, J.S. Skierski, M. Koronkiewicz, M. Mirowski, R. Wiercioch, A.P. Mazurek, Nucl. Med. Bio., 29 (2002) 169.
13. H. Brunner, K-M. Schellerer, Inorg. Chim. Acta., 350 (2003) 39.
14. A.von Braun, J. Tcherniac, Ber. Deut. Chem. Ges, 40 (1907) 2709.
15. R.P. Linstead, J. Chem. Soc., (1934) 1016.
16. A.R. Lowe, R.P. Linstead, J. Chem. Soc., (1934) 1022.
17. C.E. Dent, R.P. Linstead, J. Chem. Soc., (1934) 1027.
18. J.M. Robertson, J. Chem. Soc., (1935) 615.
19. J.M. Robertson, J. Chem. Soc., (1936) 1195.
20. C.C Leznoff, A.B.P Lever (Eds), Phthalocyanines: Properties and Applications, vol1- 4 (1991)
21. M. Calvete, G.Y. Yang, M. Hanack, Synth. Met., 141 (2004) 231.
22. P. Greory, J. Porphyrins. Phthalocyanines. 3 (1999) 468.
23. F. Rollet, S. Morlat-Thérias, J-L. Gardette, J-M. Fontaine, J. Perdereau, J-D. Polack, J. Cult. Herit., 9 (2008) 234.
24. Y.M. Rio, M.S. Rodriguez-Morgade, T. Torres, Org. Biomol. Chem., 6 (2008) 1877.
25. C. Vergnat, S. Uttiya, S. Pratontep, T. Kerdcharoen, J-F. Legrand, M. Brinkmann, Synth. Met., 161 (2011) 251.

26. A. Siejak, D. Wrobel, P. Siejak, B. Olejarz, R.M. Ion, *Dyes. Pigments*, 83 (2009) 281.
27. V. Chauke, F. Matemadombo, T.Nyokong, *J. Hazard. Mater.*, 178 (2010) 180.
28. A.K. Sarker, M.G. Kang, J-D. Hong, *Dyes. Pigments*, 92 (2012) 1160.
29. Y. Chen, N. He, J.J. Doyle, Y. Lui, X. Zhuang, W.J. Blau, *J. Photochem. Photobiol.A.*, 189 (2011) 414.
30. H. Uchida, M. Mitsui, P.Y. Reddy, S. Nakumura, T. Tou, *Arkivoc*, 11 (2005) 17.
31. P. Erk, H. Hengelsberg, *The Porphyrin Handbook: Phthalocyanine synthesis*, (Eds. K.M. Kadish, K.M. Smith. R. Guillard), Academic Press, New York, vol 19, (2003).
32. G.T. Byrne, R.P. Linstead, R.L. Lowe, *J. Chem. Soc.*, (1934) 1017.
33. N.B. McKeown, in *The Porphyrin Handbook: The synthesis of symmetrical Phthalocynine* (Eds. K.M.Kadish, K.M.Smith, R. Guillard), Academic Press, New York vol 15, (2003).
34. N.S. Nalwa, J.S. Shirk, in *Phthalocyanines: Properties and Applications*, (Eds. A.B.P. Lever, C.C. Leznoff) vol 4, (1996).
35. M. Sommerauer, C. Rager, M. Hanack. *J. Am. Chem. Soc.*, 118 (1998) 10085
36. K. Sakamoto, E. Ohno, *Prog. Org. Coat.*, 31 (1997) 139.

37. O. Dolotova, O. Kayila, Russ. J. Coord. Chem., 33 (2007) 115.
38. O. Dolotova, O. Kayila, J. Porphyrins. Phthalocyanine., 15 (2011) 632.
39. M. Gouterman, J. Mol. Spec., 6 (1961) 138.
40. J. Mack, M.J. Stillman, Coordin. Chem. Rev., 219-22 (2001) 993.
41. A. Gilbert, J. Baggot, *Essentials of molecular photochemistry*, library of congress. USA, (1995).
42. S.Fery-Forgues, D.J. Lavabre. J Chem. Ed. 76 (2001) 1260
43. J. Fu, X.Y. Li, D.K.P. Ng, C. Wu, Langmuir, 18 (2002) 3843
44. A. Ogunsipe, J. Chen, T. Nyokong. New J Chem. 28 (2004) 822
45. T.W.J GadellaJr, R.M. Clegg, T.M. Jovin, Bioimaging, 2 (1994) 139
46. X.F Wang, T. Uchida, D.M. Coleman, S. Minami., Applied Spectroscopy, 45 (1991) 360
47. X-F Zhang, H-J Xu, J. Chem. Soc. Faraday Trans., 89(18) (1993) 3347
48. H. Du, R.A. Fuh, J. Li, A. Corkan, J.S. Lindsey, Photochem. Photobiol., 68 (1998) 373
49. J. M. Dixon, M. Taniguchi, J.S. J.S. Lindsey, Photochem. Photobiol., 81 (2005) 212
50. T. H. Tran-hi, C. Desforge, C. Thiec, J.Phys. Chem., 93 (1989) 1226
51. P. Kubat, J. Mosinger, J. Photochem. Photobiol.A., 96 (1996) 93
52. S.M Bishop, A. Beeby, H. Meunier, A. W. Parker, M.S.C. Foley, D. Phillips, J. Chem. Soc. Faraday Trans., 92 (1996) 2689

53. M. Grimm, E. Eybl, M. Grabenwoger, H. Spreitzer, W. Jager, G. Grimm, P. Bock, M.M. Muller, E. Wölner, *Surg.*, 11 1 (1992) 74.
54. G. Scchurpfeil, A. Sobbi, W. Spiller, H. Kliesch, D. Wöhrle, J. Porphrin. *Phthalocyanines*. 1 (1997) 159.
55. S. Maree, T. Nyokong, J. Porphyrin. *Phthalocyanines.*, 5 (2001) 5782.
56. J. Grodkowski, J. H. Chambers, P. Neta, *J. Phys. Chem.*, 88 (1984) 5332.
57. I. Seotsanyana-Mokhosi, N. Kuznetsova, T. Nyokong, *J. Photochem. Photobiol.A: Chem.*, 140 (2001) 215.
58. S.A, Mamuru, K. I. Ozoemena, T. Fuduka, N. Kobayashi, *J. Mater Chem*. 20 (2010) 10705.
59. N. Maxakato, S. A. Mamuru, K. I. Ozeomena, *Electroanalysis* 23 (2011) 325.
60. R. A. Bulgakov, N.A. Kuznetsova, O. V. Dolotova, L.I.Solovieva, J. Mack, W.Chidawanyika, O.L. Kayila, T. Nyokong, *J. Porphyrins. Phthalocyanines.*, 16 (2012) 1217.
61. R.A. Bulgakov, N.A. Kuznetsova, O.V. Dolotova, E.N. Shevchenko, A.D. Plyutinskaya, O.L. Kaliya, T. Nyokong, *Macroheterocycles*, 5 (2012) 350
62. M. Ambroz, A. Beeby, A.J. McRobert, M.S.C. Simpson, R.K. Svnseb, D. Phillips, *J. Photochem. Photobiol. B: Biol.*, 9 (1991) 87.
63. J.R Lakowics In: *Principle of fluorescence spectroscopy* , 2nded, Kluwer Academic, New York, 1999.
64. T. Nyokong, E. Antunes in *The Handbook of Porphyrin Science*. Eds. Kadish, K. M.; Smith, K. M.; Guillard, R., Academic Press: New York World Scientific, Singapore, Vol. 7, (2010).

65. A. Ogunsipe, D. Maree, T. Nyokong, J. Mol. Struct. 650 (2003) 131.
66. J.M. Fernandes, M.D Bilgin, L.I. Grosswiener, J. Photochem. Photobiol. B: Biol., 37(1997) 131.
67. N.A. Kuznetsova, N.S. Gretsova, V.M. Derkacheva, S.A.Mikhaleenko, L.I. Solov'eva, O.A Yuzhalova, O.L. Kaliya, E.A. Luk'yanets, Russ. J. Gen. Chem., 72 (2001) 300.
68. Sun, S. Anders, T. Thomson, J. E. E. Baglin, M. F Toney, H. F. Hamann, C.B. Murray, J. Phys. Chem. B., 107 (2003) 5419.
69. B. N. Achar , K. S. Lokesh, J. Organomet. Chem., 689 (2004) 2601.
70. M. Fujiki, H. Tabei, Langmuir, 4 (1988) 320.
71. A. W. Snow, J. R. Griffith, N. P. Marullo, Macromolecules, 17 (1984) 1614.
72. S. Sapra, D. D. Sarma, Pramana, 65 (2005) 565.
73. M.S. Antonious Spectrochim. Acta. A., 53 (1997) 317.
74. T. Forster, G. Hoffmann, J. Phys. Chem., 71 (1971) 63.
75. M. Idowu, T. Nyokong, J. Photochem. Photobiol.A., 200 (2008) 396.
76. K. Ishii, N. Kobayashi, in: K.M. Kadish, K.M. Smith, R. Guillard, (Eds.), Porphyrin Handbook, *Academic Press.*, New York, 2003, vol. 16.
77. A. Kotiaho, R. Lahtinen, A. Efimov, H. K. Metsberg, E. Sariola, H. Lehtivuori, N. V. Tkachenko, H. Lemmetyinen,, J. Phys. Chem.C., 114 (2010) 162.

